

AD-A053 765

TECHNOLOGY INC SAN ANTONIO TEX LIFE SCIENCES DIV
OCULAR HAZARDS OF PICOSECOND AND REPETITIVE-PULSED LASERS. VOLU--ETC(U)
APR 78 H W HEMSTREET, J S CONNOLLY F41609-73-C-0016

UNCLASSIFIED

TI-77-0564-03

SAM-TR-78-20

NL

| OF |
AD
A053 765



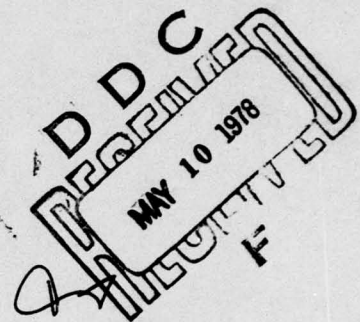
AD A 053765

Report SAM-TR-78-20

2

OCULAR HAZARDS OF PICOSECOND AND REPETITIVE-PULSED LASERS

Volume I: Nd:YAG Laser (1064 nm)



AU NO. _____
DDC FILE COPY

H. W. Hemstreet, Jr., Ph.D.

J. S. Connolly, Ph.D.

D. E. Egbert, Captain, USAF (USAFSAM/RZL)

Technology Incorporated

511 West Rhapsody Drive

San Antonio, Texas 78216

April 1978

Final Report for Period 16 February 1973 - 15 February 1976

Approved for public release; distribution unlimited.

Prepared for

USAF SCHOOL OF AEROSPACE MEDICINE

Aerospace Medical Division (AFSC)

Brooks Air Force Base, Texas 78235



NOTICES

This final report was submitted by Technology Incorporated, 511 West Rhapsody Drive, San Antonio, Texas 78216, under contract F41609-73-C-0016, job order 7757-02-33, with the USAF School of Aerospace Medicine, Aerospace Medical Division, AFSC, Brooks Air Force Base, Texas. Major Jack A. Labo (SAM/RZL) was the Laboratory Project Scientist-in-Charge.

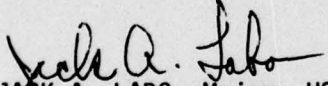
When U.S. Government drawings, specifications, or other data are used for any purpose other than a definitely related Government procurement operation, the Government thereby incurs no responsibility nor any obligation whatsoever; and the fact that the Government may have formulated, furnished, or in any way supplied the said drawings, specifications, or other data is not to be regarded by implication or otherwise, as in any manner licensing the holder or any other person or corporation, or conveying any rights or permission to manufacture, use, or sell any patented invention that may in any way be related thereto.

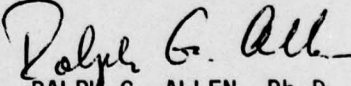
The animals involved in this study were procured, maintained, and used in accordance with the Animal Welfare Act of 1970 and the "Guide for the Care and Use of Laboratory Animals" prepared by the Institute of Laboratory Animal Resources - National Research Council.

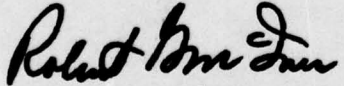
The views expressed herein do not necessarily reflect the views of the USAF School of Aerospace Medicine, the U.S. Air Force, or the Department of Defense.

This report has been reviewed by the Information Office (OI) and is releasable to the National Technical Information Service (NTIS). At NTIS, it will be available to the general public, including foreign nations.

This technical report has been reviewed and is approved for publication.


JACK A. LABO, Major, USAF
Project Scientist


RALPH G. ALLEN, Ph.D.
Supervisor


ROBERT G. MCIVER
Brigadier General, USAF, MC
Commander

UNCLASSIFIED

SECURITY CLASSIFICATION OF THIS PAGE (When Data Entered)

REPORT DOCUMENTATION PAGE		READ INSTRUCTIONS BEFORE COMPLETING FORM	
1. REPORT NUMBER SAM-TR-78-20		2. GOVT ACCESSION NO. TI-77-0564-03	
3. TITLE (and Subtitle) OCULAR HAZARDS OF PICOSECOND AND REPETITIVE-PULSED LASERS. Volume I. Nd:YAG Laser (1064 nm).		4. TIME OF REPORT & PERIOD COVERED Final Report. 16 Feb 73 - 15 Feb 76.	
5. AUTHOR(s) H. W. Hemstreet, Jr. J. S. Connolly D. E. Egbert		6. PERFORMING ORG. REPORT NUMBER 77-0564-03	
7. PERFORMING ORGANIZATION NAME AND ADDRESS Technology Incorporated Life Sciences Division 511 West Rhapsody Drive San Antonio, Texas 78216		8. CONTRACT OR GRANT NUMBER(s) F41609-73-C-0016	
9. CONTROLLING OFFICE NAME AND ADDRESS USAF School of Aerospace Medicine (RZL) Aerospace Medical Division (AFSC) Brooks Air Force Base, Texas 78235		10. PROGRAM ELEMENT, PROJECT, TASK AREA & WORK UNIT NUMBERS 622025 7757-02-33	
11. MONITORING AGENCY NAME & ADDRESS (if different from Controlling Office)		12. REPORT DATE Apr 78	
		13. NUMBER OF PAGES 46	
		14. SECURITY CLASS. (of this report) Unclassified	
		15a. DECLASSIFICATION/DOWNGRADING SCHEDULE 12 47 P.	
16. DISTRIBUTION STATEMENT (of this Report) Approved for public release; distribution unlimited.			
17. DISTRIBUTION STATEMENT (of the abstract entered in Block 20, if different from Report) D D C FORM 12 MAY 10 1978 RECEIVED F			
18. SUPPLEMENTARY NOTES			
19. KEY WORDS (Continue on reverse side if necessary and identify by block number) Laser-induced retinal damage/rhesus monkey Photobiological damage mechanisms ND-YAG laser, Q-switched Ocular damage thresholds Single-pulse thresholds Thermal damage mechanisms Repetitive-pulse thresholds			
20. ABSTRACT (Continue on reverse side if necessary and identify by block number) Retinal damage thresholds are discussed for exposure of rhesus maculae to continuous wave and repetitive-pulse trains of 1064-nm Nd:YAG laser radiation. For all single-pulse exposures and for repetitive pulses contained within a 0.05-sec train, retinal damage appears to be induced primarily by thermal mechanisms. For the longer pulse-train durations, a cumulative effect is apparent when the repetition frequencies are in the range of >1 to <100 Hz. Experiments were conducted in such a way that direct comparisons could be made with previous data and that accumulated results could be compiled into a self-consistent empirical model.			

DD FORM 1 JAN 73 1473

EDITION OF 1 NOV 65 IS OBSOLETE

UNCLASSIFIED

SECURITY CLASSIFICATION OF THIS PAGE (When Data Entered)

407 650

SUMMARY

This volume discusses retinal damage thresholds for exposures of the maculae of rhesus monkeys (*Macaca mulatta*) to continuous-wave (CW) and repetitive-pulse trains of Nd:YAG laser radiation at 1064 nm. The laser was operated in the TEM₀₀ mode with a full angle beam divergence of ≤ 1.2 mrad and a $1/e^2$ beam diameter of ≤ 1.5 mm at the corneal plane.

Single-pulse exposures were made at pulsewidths of 270 nsec and 0.5 and 5 sec. Repetitive-pulse exposures were made for combinations of Q-switched pulses with train durations of 0.05, 0.5, 5 and 30 sec at pulse repetition frequencies from 0.1 Hz to 10 kHz. Nominal pulsewidths were 300 (± 25) nsec except at the highest repetition rate where ~ 730 -840 nsec pulses were obtained.

For each threshold measurement at least ten eyes were exposed at each of sixteen macular sites and were examined ophthalmoscopically at one hour post-exposure. A simple lesion/no-lesion determination was made and the damage thresholds (ED50) were calculated by the method of probits. Threshold powers are expressed in terms of peak pulse power at the cornea. For all single-pulse exposures and for repetitive pulses contained within a train of 0.05 sec, retinal damage appears to be induced primarily by thermal mechanisms. That is, the observed data show good agreement with calculations of the Illinois Institute of Technology Research Institute (IITRI) thermal model, though rather large retinal image sizes must be assumed.

In contrast, for the longer pulse-train durations, there is an apparent cumulative effect of repetitive, Q-switched pulses when the repetition frequencies are in the range of ≥ 1 to ≤ 100 Hz. For example, the retina is more sensitive to double-pulse exposures, by a factor of 5 to 10 relative to single-pulse thresholds, when the interpulse spacing is ~ 0.2 sec.

Non-thermal damage mechanisms appear to be involved. Because of the stark similarity between our near-IR and visible repetitive pulse data (see Volume II) we tend to favor a damage mechanism of photobiological or photochemical origin, possibly involving the photoreceptors themselves. Evidently, single photon photochemistry in the near-IR presents serious problems in terms of realistic hypotheses regarding the nature of the chromophores. Accordingly, we *tentatively* invoke frequency doubling in the anterior ocular media and/or biphotonic absorption of near-IR photons in the retina to explain our results. In either case, the quantum efficiency need be only $\sim 0.1\%$ in order to achieve quantitative agreement with retinal irradiances typical of our visible laser experiments (see Volume II).

However, it must be borne in mind that this hypothesis of photochemical damage, resulting from non-linear photon processes, remains to be tested; other mechanisms, such as membrane disruption by acoustic shock waves or a combination of effects, including thermal processes, are not ruled out. For that matter, our present understanding of the fundamental biochemical and biophysical mechanisms involved in thermal damage of the retina can best be termed rudimentary. Thus, we likewise do not rule out strictly thermal damage processes of a type hitherto unencountered in laser ocular hazards research.

PREFACE

The authors wish to recognize the superb technical assistance of Ms. Kathleen K. Altobelli, Mr. J. Michael Scott, and Mr. Charles C. Stevens given in support of this three-year study. We thank Mr. John E. McGlothan, III and Mr. Gregory L. Sweeney for preparing the figures, and Mrs. Maribeth Bains and Mrs. Sharon Johnson for typing the various drafts of the manuscripts.

We also thank Mr. Richard C. McNee, USAFSAM Biometrics Division, for carrying out the many probit analyses reported here and for his critical review of the manuscript. Very helpful discussions with Dr. Joseph A. Zuclich, Dr. J. Terry Yates, Major Jack A. Labo, and Lieutenant Colonel William D. Gibbons are also gratefully acknowledged.

Our highest praise and deepest gratitude are reserved for Mr. W. Robert Bruce, without whose expertise and assistance this program could not have been completed. Mr. Bruce evaluated all of the more than 12,000 retinal exposures made in this study. The precision of the data is an eloquent tribute to his remarkable skills, his long experience, and his professional objectivity.

TABLE OF CONTENTS

Page

INTRODUCTION-----	5
OBJECTIVES-----	7
PRIMATE CARE AND PREPARATION-----	9
APPARATUS AND CALIBRATION-----	9
Experimental Apparatus-----	9
System Calibration and Measurement of Beam Parameters-----	12
Laser Power Measurements-----	12
Pulsewidth Measurements-----	14
Laser Beam Divergence-----	14
EXPERIMENTAL PROCEDURES-----	14
RESULTS-----	19
DISCUSSION-----	27
General Observations-----	27
Thermal Model Calculations-----	29
Working Hypotheses to Explain Cumulative Effects of Repetitive Laser Pulses-----	33
REFERENCES-----	39
BIBLIOGRAPHY-----	43
APPENDIX A: DATA ANALYSIS-----	45

LIST OF FIGURES

1. Block diagram of experimental apparatus-----	11
2. Block diagram of laser power calibration system-----	13
3. Oscilloscope traces of repetitive, Q-switched Nd:YAG laser pulses-----	15
4. Spatial intensity profiles of Nd:YAG laser beam in near (13.5 cm) and far (210 cm) fields-----	16
5. Diagram of macular exposure sites on rhesus retina-----	18
6. Experimental single-pulse retinal thresholds for Nd:YAG laser exposures (1064 nm)-----	21
7. Summary of retinal threshold data for repetitive Q-switched Nd:YAG laser pulses (1064 nm)-----	23
8. Retinal threshold vs. pulse separation for fixed numbers of Q-switched Nd:YAG laser pulses-----	26
9. Observed retinal thresholds vs. repetition rate for 0.05-30-sec trains of 10-μsec, 514.5-nm laser pulses-----	30
10. Retinal threshold vs. pulse separation for fixed numbers of repetitive 10-μsec, 514.5-nm laser pulses-----	31
11. Idealized interpulse power dependencies predicted by working hypotheses for double-pulse threshold experiments-----	37

LIST OF TABLES

1. Single-pulse retinal damage thresholds at 1060 nm-----	20
2. Summary of ED50 thresholds for rhesus maculae exposed to repetitive, Q-switched 1064-nm laser pulses-----	22
3. Measured and interpolated thresholds for 2- and 5-pulse exposures at various separations of 300 nsec Nd:YAG pulses-----	25
4. Comparative peak retinal temperatures predicted by IITRI thermal model at threshold powers for 514.5- and 1064-nm laser pulses-----	32
5. Threshold powers and energies for repetitive, 10-μsec, 514.5-nm laser pulses at optimum spacing-----	35

ACCESSION FOR	
NTIS	Section <input checked="" type="checkbox"/>
DDC	B. H. Section <input type="checkbox"/>
UNANNOUNCED	<input type="checkbox"/>
JUSTIFICATION	
BY	
DISTRIBUTION/AVAILABILITY CODES	
Dist.	SPECIAL
A	

OCULAR HAZARDS OF PICOSECOND AND REPETITIVE-PULSED LASERS
VOLUME I: Nd:YAG LASER (1064 nm)

INTRODUCTION

Deleterious thermal effects resulting from exposure of biological tissues to intense light sources have been actively studied for a number of years (1-6). Nuclear detonations and lasers are among the most intense man-made sources of optical radiation and present serious hazards to the eye and the skin.

The eye has been recognized as particularly susceptible to damage caused by exposure to direct or specularly reflected radiation, both thermal (7-12) and optical (13-34). The proliferation of lasers for military, industrial and scientific purposes has made it mandatory to develop practical safety criteria and standards to govern their operation. One principal objective of this study was to contribute to this development in the area of picosecond and repetitive laser pulses.

Ocular damage is most likely to occur either in the cornea and lens or in the chorioretinal region of the eye, depending on the wavelength of the laser radiation. In the ultraviolet (UV) region of the spectrum, most of the incident radiation is absorbed by the cornea and/or lens and very little reaches the retina (35-37). However, in the visible and near infrared (IR), the cornea and lens are relatively transparent (36,37) allowing a large percentage of the radiation to be transmitted to the chorioretinal region, where it then undergoes substantial absorption, in some cases as much as 85% (38).

The mechanisms responsible for UV-induced damage in the corneal epithelium are predominantly photochemical (39,40). Retinal damage from laser radiation in the visible or near-IR region, on the other hand, is presumed to be the result of a temperature increase (1-6, 9-12, 21, 22, 30, 41-43) induced by absorption of the optical radiation in the pigment epithelium and other chorioretinal layers. The damage, centered about the region of maximum temperature rise, is thought to involve thermal protein denaturation or enzyme inactivation (3).

Biological tissue is able to maintain normal viability only within a relatively narrow temperature range; therefore, it is not unreasonable to expect that small temperature increases in the retina might cause tissue damage. Both the damage itself and the rates of the damage processes are considered to be temperature dependent. Thus, ultimate production of damage must be considered in terms of thermally accelerated, biochemical rate processes. As such, the laser intensity required to produce threshold damage is best estimated by a temperature-time integration taken over an effective exposure time.

Theoretical thermal models based on these concepts have been constructed. A model currently used by the USAF School of Aerospace Medicine was developed by Takata and co-workers (44) at the Illinois Institute of Technology Research Institute (IITRI), and is commonly referred to as the IITRI model. This sophisticated computer routine represents a significant improvement over earlier models and was designed specifically to account for laser-induced ocular damage.

Its purpose is to provide the capability of predicting ocular damage thresholds over a wide range of laser parameters and exposure conditions.

An important factor in chorioretinal absorption and damage is that the irradiance (intensity/unit area) of the light that strikes the retina can be as much as 10^5 times greater than the irradiance at the cornea because of the focusing properties of the eye and the high degree of laser beam collimation (for example, see reference 30). Therefore, the eye can incur retinal damage from relatively low power lasers operating in the visible and near-IR regions of the spectrum. Since laser radiation is nearly invisible in clear air except when viewed directly along the propagation axis, personnel in the vicinity of an operating laser could be unaware of the radiation and thus have little warning before receiving a direct or specularly reflected pulse in the eye.

This study is concerned with maximum permissible exposure levels (MPE) with regard to retinal damage. At present the minimum, or threshold, damage is defined in terms of the minimum lesion that can be detected with a clinical ophthalmoscopic instrument. The lesion itself is defined as a perceptible retinal discoloration, usually a white or grayish area surrounded by a dark area. Laser-induced retinal lesions usually have the shape and symmetry of the focused laser spot which, in virtually all cases, is circular.

Allen and co-workers (10) studied the effect of focused spot size on retinal lesion threshold, using a non-coherent source, and found that for a given corneal irradiance, smaller retinal spot sizes produced lower thresholds. This was confirmed by King and Geeraets (28) using a Q-switched ruby laser source. Clarke (29) and Sliney (30) considered the problems relevant to quantifying laser ocular hazards and developing laser safety criteria. Vassiliadis et al. (18) performed laser beam retinal threshold measurements and discussed the problems of theoretical predictions of the retinal temperatures produced and the relation between temperature and tissue damage in terms of rate processes.

Recent experiments, by and large, have dealt with worst-case conditions to produce threshold damage; i.e., a laser operating in the TEM₀₀ mode (minimum beam divergence) with a beam cross-section that has a radially symmetric, Gaussian distribution. This condition also implies that the subject eye is in the unaccommodated state and has no refractive error, so that the impinging beam is focused to a minimum spot size (maximum irradiance) on the retina.

Dunsky and Lappin (14) measured paramacular thresholds of primates using worst-case parameters with a krypton-ion laser emitting at 568.2 nm. The laser was operated in the TEM₀₀ mode with a beam divergence of 0.8 milliradians (mrad). Ophthalmic corrective lenses were used as needed to compensate for refractive error. Bresnick et al. (15) performed similar worst-case threshold measurements on primate maculae. They used an argon-ion laser emitting at 514.5 nm in the TEM₀₀ mode with a divergence of 0.7 mrad, and they also corrected the subject eye for refractive error. In addition to clinical observations, they found histopathologic evidence of damage at exposure levels below the thresholds as determined ophthalmoscopically.

Ham et al. (16) used a helium-neon laser at 632.8 nm wavelength with a divergence of 0.7 mrad in the TEM₀₀ mode to expose the macular area. They reported a large variation of the retinal image size (50 to 200 μm) over the population of subject eyes. Apparently they did not correct the eyes for refractive or chromatic errors.

Frisch and co-workers (17) carried out a comparative study of retinal thresholds using a Q-switched ruby laser (694.3 nm) and an argon-ion laser (514.5 nm). Each was operated in its lowest order mode (TEM₀₀), but the divergence of the ruby was slightly higher (1 mrad) than that of the argon (0.7 mrad). Lenses were used to correct for refractive error and chromatic difference between argon and ruby. Histopathologic examinations of suprathreshold exposure sites revealed definite differences in the type of damage caused by the short-duration Q-switched ruby pulses (30-nsec pulsewidths) and the much longer argon-ion pulses (12- to 125-msec pulsewidths). At intensities on the order of 10 times threshold levels, the damage produced by the Q-switched ruby pulses was observed to be considerably more extensive than that produced by the argon-ion pulses. Also, a comparison was made between thresholds obtained for the macular and paramacular regions using single, long pulses from the argon-ion laser. Lower thresholds were found for the macular region, which can probably be attributed to the higher absorption cross-sections of the macular pigments (23).

The above studies were concerned with single-pulse laser exposures at visible wavelengths; more recent investigations have considered also the effects of repetitive-pulse exposures in the visible and near-IR regions. Skeen et al. (20,24) measured macular thresholds under worst-case conditions using repetitive pulse-train exposures from an argon-ion laser (514.5 nm) and a Q-switched Nd:YAG laser (1064 nm). Expressing thresholds in terms of either energy per pulse or peak pulse power, they reported evidence for a cumulative effect. Specifically, the energy per pulse required to produce a threshold lesion was found to decrease as the total number of pulses in the exposure train was increased. Gibbons and Egbert (27), using an argon-ion laser (514.5 nm), reported similar results for several combinations of repetition frequencies, pulsewidths and total pulse-train durations. Ebberts and Dunskey (31) studied rhesus paramacular thresholds produced by Q-switched Nd:YAG laser and also noted evidence for a slight cumulative effect. These investigations were concerned with retinal threshold measurements under worst-case conditions and all used essentially the same criterion for determining when damage had occurred, namely the appearance of an ophthalmoscopically visible lesion at the exposure site within one hour after irradiation.

The present program was specifically designed to investigate damage thresholds in the rhesus macula for two different laser wavelengths (514.5 nm and 1064 nm), using worst-case conditions over a broad range of pulsewidths, pulse-repetition rates and pulse-train durations. This first volume of the final report deals exclusively with the near-IR studies.

OBJECTIVES

The objectives of the program were three-fold: (1) to acquire additional experimental threshold data for retinal damage induced by trains of repetitive laser pulses; (2) to construct an empirical model of such damage; and (3) to validate and help define limits of applicability of the IITRI thermal model (44) of retinal damage induced by repetitive-pulse exposures.

As in many previous investigations (14-20, 23-28, 30-34, 39-43), all of the experiments reported here were performed *in vivo* on the eyes of young rhesus monkeys (*Macaca mulatta*). There is evidence (18) that threshold measurements based on paramacular exposures yield higher values than those based on macular

exposures; therefore in this study, all test exposures were placed within the macula and generally away from the *fovea centralis*. The anatomy, physiology and optical properties of the rhesus eye are very similar to those of the human eye; thus, for purposes of ocular hazard evaluations, the rhesus eye can be considered as a scaled-down version of the human eye. In addition, the detailed thermal and optical absorption coefficients of rhesus ocular media have been measured *in vitro* (35-38, 41-43) and these measurements provide parameters for developing thermal models that can be tested against the rapidly accumulating ocular-damage data obtained from *in vivo* experiments on the rhesus.

The damage threshold, ED50, is a statistically determined value calculated from exposure data generally taken from ten or more test eyes. This value represents the pulse power (or energy) incident on the cornea, that has a 50% probability of inducing macular damage in an eye selected at random from the subject population. For a given laser with fixed optical parameters (wavelength, beam divergence, mode structure, etc.), the threshold, expressed in terms of pulse power incident on the cornea of an eye focused at infinity, is a function of pulsewidth, pulse-repetition rate and pulse-train duration. Therefore, threshold measurements were performed using selected values of the above variables over a wide range compatible with state-of-the-art commercial laser equipment.

Since a large body of retinal threshold data has been acquired in prior research at other laboratories, experiments in the present program were conducted in such a way that direct comparisons could be made with previous data and that the accumulated results could be compiled into a self-consistent empirical model. Insofar as possible, the experimental parameters and criteria used in much of the previous work were adopted in this program as follows:

- (1) The subjects used were young rhesus monkeys (*Macaca mulatta*) ranging in age from two to four years and in weight from two to four kg. No distinction was made between male and female subjects.
- (2) Only the macular region of the retina was irradiated for purposes of damage determination.
- (3) Damage was defined as the appearance of a lesion at the exposed site within one hour after irradiation.
- (4) A lesion was defined as an ophthalmoscopically visible, dark, circular discoloration containing a white or light-gray center.
- (5) Each macula was exposed at 16 different sites, with a range of intensities (laser beam power) varying over a log-normal distribution above and below the estimated threshold intensity.
- (6) In all but two cases, a minimum of ten eyes was irradiated at a given set of laser parameters to determine the threshold under those conditions.
- (7) The laser was operated in its lowest order Fabry-Perot mode (TEM_{00}) with a diffraction-limited beam divergence.
- (8) The laser power was taken to be the total energy in the beam (measured at the corneal plane) divided by the effective pulsewidth.

- (9) An ophthalmic lens was used if the subject eye had a refractive error greater than ± 0.5 diopter in any meridian.
- (10) All retinal examinations were made by the same person.

The data reported here are for a Nd:YAG laser operating at its fundamental frequency (1064 nm) in either the continuous-wave (CW) or Q-switched mode. In the CW mode, single-pulse exposure times were 0.5 to 5.0 sec; in the Q-switched mode, pulse-repetition rates and exposure times were varied from DC (i.e., single pulse) to 10 kHz and from 0.05 to 30 sec, respectively. Q-switched pulses were generally ~ 300 nsec duration except at the highest repetition frequencies, where pulsewidths were ~ 730 to 840 nsec.

PRIMATE CARE AND PREPARATION

The San Antonio Laboratory of Technology Incorporated is equipped with a controlled environment vivarium which is used exclusively for housing infrahuman primates to be employed as research subjects. Both temperature and humidity were carefully controlled and the primates were individually housed in stainless steel cages. Daily care and feeding were performed by trained personnel. Regular inspections were made by a representative of the U.S. Department of Agriculture, Agricultural Research Service, Animal Health Division, as well as by a company-retained veterinarian.

On the day prior to the retinal irradiations of a primate, atropine sulfate (1% ophthalmic ointment) was introduced into each conjunctival sac to achieve maximum pupillary dilation. Approximately one hour prior to retinal irradiation, each subject was tranquilized with an intra-muscular injection of phencyclidine hydrochloride (Sernylan), 20 mg/cm³, at a dosage of 1 mg/kg of body weight. After onset of tranquilization, a 19-gauge intravenous catheter was inserted into a posterior superficial vein in one leg. To initiate anesthetization, 0.5 cm³ of sodium pentobarbital (50 mg/cm³) was administered by way of the intracatheter. Smaller increments, 0.1 cm³ or less, were injected as necessary to maintain both constant core temperature and deep anesthesia, up to a maximum total dose of 1 cm³/kg of body weight. The eyelids were held open by means of a stainless steel speculum during retinal exposures. Since lacrimation is usually suppressed by anesthesia, the eye was irrigated frequently with sterile, normal saline to preserve corneal transparency. Throughout the course of the experiment, the primate core temperature was monitored with a Yellow Springs Instruments model 702 telethermometer equipped with a model 402 rectal probe. The subjects were wrapped securely in a heated blanket and core temperatures were maintained at $97^{\circ} \pm 2^{\circ}\text{F}$ ($36^{\circ} \pm 1^{\circ}\text{C}$).

APPARATUS AND CALIBRATION

Experimental Apparatus

A Coherent Radiation model 60 Nd:YAG laser emitting at 1064 nm in the TEM₀₀ mode was used. The laser could be operated either in the continuous-wave (CW) or Q-switched mode. In the latter case, a model 460 acousto-optic device was used which permitted generation of either individual Q-switched pulses or repetitive trains of pulses at frequencies continuously variable from 50 kHz down

to 500 Hz. For lower pulse repetition frequencies, the internal frequency oscillator was by-passed and the Q-switch cell was triggered by an externally coupled Systron-Donner Datapulse model 115 pulse generator. This unit, which in turn was coupled to a Tektronix type 162 waveform generator, provided pulse-repetition frequencies as low as 0.1 Hz and pulse-train durations ranging from 0.05 to 30 sec.

In the Q-switched mode, pulsewidths are determined by the physical characteristics of the Nd:YAG rod and the optical pumping scheme. Measurements over the frequency range spanned by this study showed that for frequencies from DC to about 500 Hz, pulsewidths as short as 270 nsec could be achieved. At 1-2 kHz this broadened slightly to about 300 nsec and at higher frequencies the pulsewidth varied appreciably with increasing repetition rate, up to ~730-840 nsec at 10 kHz.

Laser pulses were monitored by a photodiode (EG&G YAG 444), the output of which was DC-coupled to a wide bandwidth oscilloscope (Tektronix type 555 or 7633) for on-line determination of pulsewidth, intensity and repetition rate. This was accomplished in the usual way by splitting off a small fraction of the laser beam with a thin optical flat and directing the reflected portion to the photodiode as shown in Figure 1. Since the fraction of light intensity was directly proportional to the intensity of the main beam impinging on the cornea, the photodiode could be calibrated so that its peak output in volts as read on the oscilloscope was a direct measure of the peak pulse power in Watts.

For the Q-switched, repetitive-pulse exposures, the pulse-train duration was varied from 0.05 to 30 sec, by means of an appropriate gate pulse fed into the pulse generator from the Tektronix waveform generator. The error of the gate pulse length, and hence of the pulse-train duration, was less than $\pm 0.5\%$ as determined by measuring the total train length using an appropriate time-base sweep of the oscilloscope.

For the 0.5- and 5-sec single-pulse exposures, the laser was operated in the CW mode and the respective pulses to the eye were obtained by externally gating the beam on and off with a Vincent shutter. The repeatability of this electro-mechanical device was found to deviate from its set aperture time by less than $\pm 4\%$ as determined from oscilloscope measurements.

Pulse powers at the cornea were varied by adjusting the current of the excitation lamps and by interposing either a fixed 5 x 5 cm neutral density filter or an Inconel-coated Kodak circular neutral density wedge (range 0-2 OD) in the laser beam. The circular wedge was tilted at a large angle from the normal in order to minimize interference between the transmitted beam and the second-surface reflections off the Inconel coating.

Visual examination of each primate retina was performed with a Zeiss fundus camera rigidly mounted with its optic axis perpendicular to the laser beam (Fig. 1). This ophthalmoscopic device was used to view the primate retinae for proper placement of the test exposures and for post-exposure examination to determine which of the irradiated sites incurred damage.

Each primate subject was held in a prone position on a mechanically adjustable table mount adjacent to the fundus camera, with ear bars holding the head rigid in an upright position. The pupil of the subject eye was positioned with respect to the camera and laser beam axis by one or more of the five mechanical adjustments on the table mount (x, y, z, azimuth and elevation).

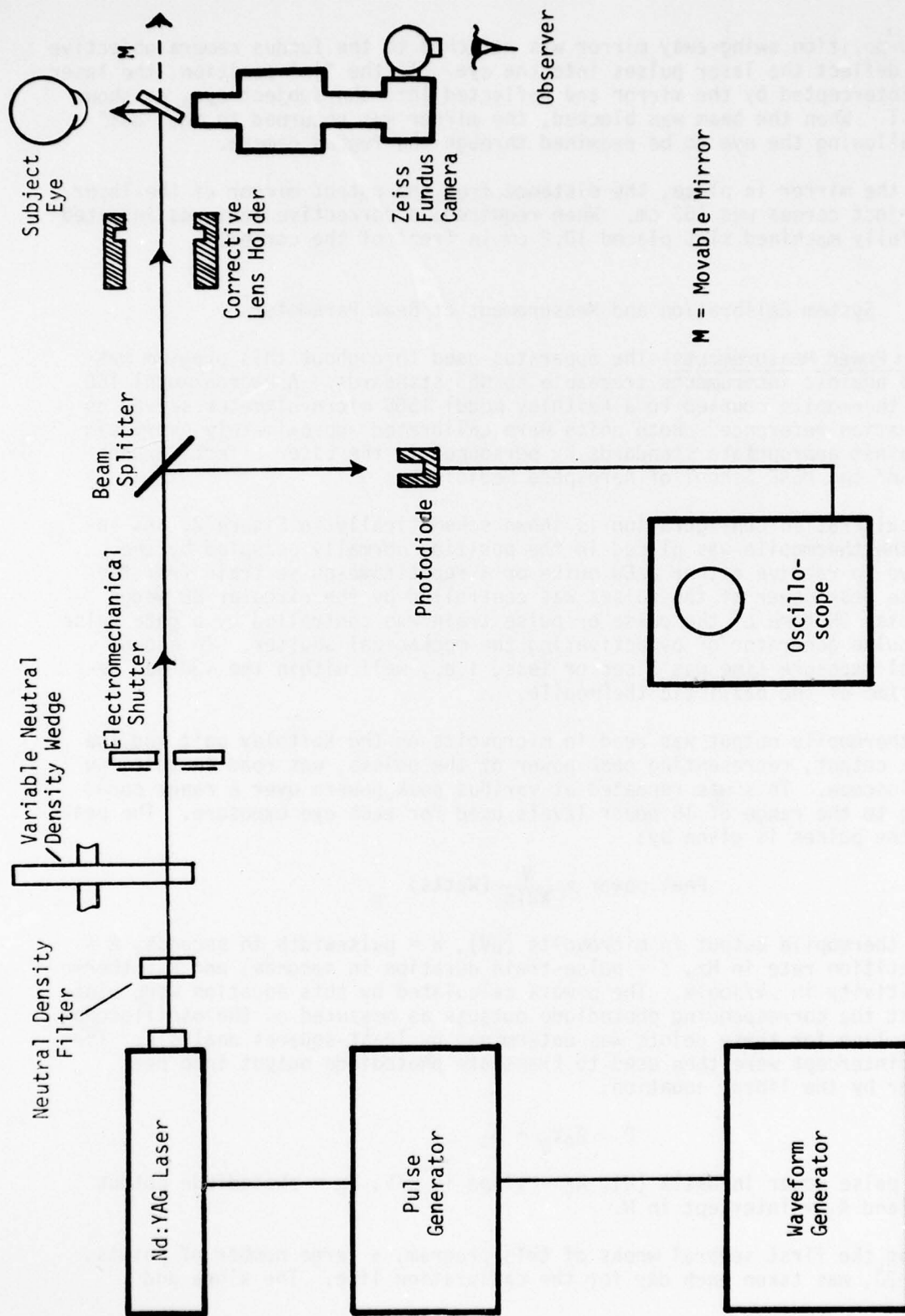


Figure 1. Block diagram of experimental apparatus.

A two-position swing-away mirror was attached to the fundus camera objective barrel to deflect the laser pulses into the eye. In the "in" position, the laser beam was intercepted by the mirror and deflected into the subject eye, as shown in Figure 1. When the beam was blocked, the mirror was returned to the "out" position allowing the eye to be examined through the fundus camera.

With the mirror in place, the distance from the output mirror of the laser to the subject cornea was 103 cm. When required, a corrective lens was inserted in a carefully machined slot placed 10.2 cm in front of the cornea.

System Calibration and Measurement of Beam Parameters

Laser Power Measurements--The apparatus used throughout this program was calibrated against instruments traceable to NBS standards. A Hadron model 100 ballistic thermopile coupled to a Keithley model 150B microvoltmeter served as the calibration reference. Both units were calibrated approximately every six months against appropriate standards by personnel in the Laser Effects Branch (SAM/RZL) of the USAF School of Aerospace Medicine.

The calibration configuration is shown schematically in Figure 2. As indicated, the thermopile was placed in the position normally occupied by the primate eye to receive either a CW pulse or a repetitive-pulse train from the laser. The peak power of the pulses was controlled by the circular ND wedge and the total ON time of the pulse or pulse train was controlled by a gate pulse from the pulse generator or by activating the mechanical shutter. In either case, total exposure time was 3 sec or less, i.e., well within the ~30 sec relaxation-time of the ballistic thermopile.

The thermopile output was read in microvolts on the Keithley unit and the photodiode output, representing peak power of the pulses, was read in volts on the oscilloscope. This was repeated at various peak powers over a range corresponding to the range of 16 power levels used for each eye exposure. The peak power of the pulses is given by:

$$\text{Peak power} = \frac{V}{WRTK} \text{ (Watts)}$$

where V = thermopile output in microvolts (μV), W = pulsewidth in seconds, R = pulse-repetition rate in Hz, T = pulse-train duration in seconds, and K = thermopile sensitivity in $\mu\text{V}/\text{joule}$. The powers calculated by this equation were plotted against the corresponding photodiode outputs as measured on the oscilloscope. A best-fit line for these points was determined by least-squares analysis. The slope and intercept were then used to translate photodiode output into peak pulse power by the linear equation:

$$P = A_0 V_p + A_1$$

where P = pulse power in Watts (W), A_0 = slope in W/V, V_p = photodiode output in volts, and A_1 = intercept in W.

During the first several weeks of this program, a large number of points, typically 20, was taken each day for the calibration line. The slope and

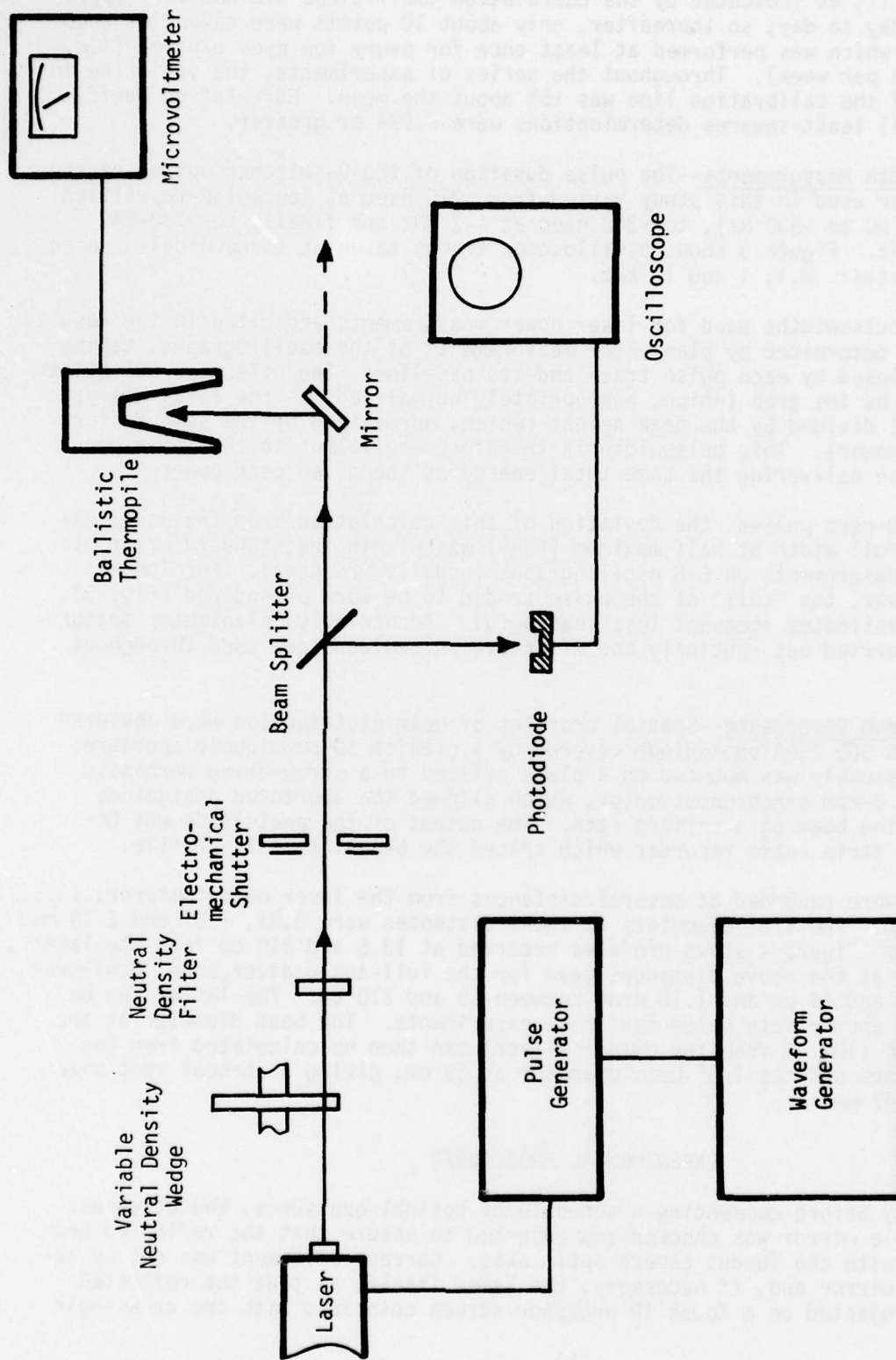


Figure 2. Block diagram of laser power calibration system.

closeness of fit as indicated by the correlation coefficient did not vary appreciably from day to day; so thereafter, only about 10 points were taken for each calibration, which was performed at least once for every ten eyes exposed (i.e., at least once per week). Throughout the series of experiments, the variation in slope (A_0) of the calibration line was $\pm 5\%$ about the mean. Correlation coefficients for all least-squares determinations were 0.994 or greater.

Pulsewidth Measurements--The pulse duration of the Q-switched output of the Nd:YAG laser used in this study varied from ~ 270 nsec at low pulse-repetition frequencies (DC to ~ 500 Hz), to ~ 300 nsec at 1-2 kHz and finally to ~ 730 -840 nsec at 10 kHz. Figure 3 shows oscilloscope traces taken at three widely spaced repetition rates: 0.1, 1 and 10 kHz.

Actual pulsewidths used for laser power measurements and cited in the Results section were determined by planimeter measurements of the oscillographs, taking the area enclosed by each pulse trace and its baseline. The effective pulsewidth was taken to be the area (which, appropriately normalized, is the total energy of the pulse) divided by the peak height (which, normalized by the same factor, is the peak power). This pulsewidth is therefore equivalent to that of a rectangular pulse delivering the same total energy at the given peak power.

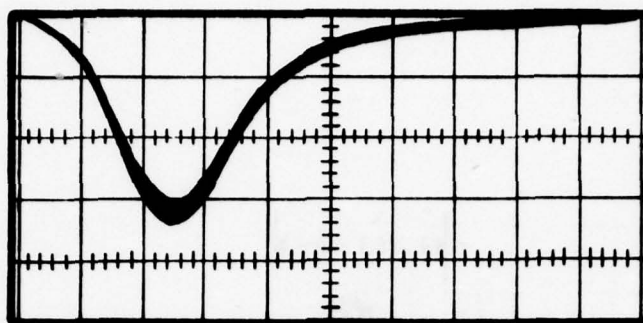
For ~ 300 -nsec pulses, the deviation of this calculation from the usual expression of full width at half maximum (FWHM) was within the standard error of planimeter measurements on 6-8 oscillographs (usually ~ 25 nsec). For longer pulses, however, the "tail" of the pulse tended to be more pronounced (Fig. 3), making FWHM estimates somewhat less meaningful. Accordingly, planimeter measurements were carried out routinely and effective pulsewidths are used throughout this report.

Laser Beam Divergence--Spatial profiles of beam distribution were measured using an EG&G SGD 100A photodiode covered by a precise $50\text{-}\mu\text{m}$ pinhole aperture. The entire assembly was mounted on a plate affixed to a screw-drive mechanism powered by a 2-rpm synchronous motor, which allowed the apertured photodiode to traverse the beam at a uniform rate. The output of the photodiode was DC-coupled to a strip chart recorder which traced the beam-intensity profile.

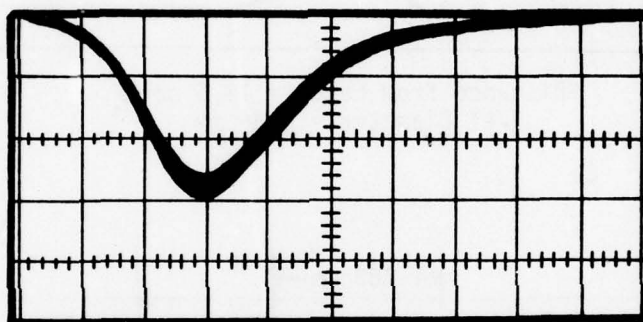
Traces were recorded at several distances from the laser output mirror: 13.5, 69 and 210 cm. The $1/e^2$ diameters at these distances were 0.84, 1.07 and 2.73 mm, respectively. Figure 4 shows profiles recorded at 13.5 and 210 cm from the laser. Calculations at the above distances gave for the full-angle divergence, 0.41 mrad between 13.5 and 69 cm and 1.18 mrad between 69 and 210 cm. The latter can be taken as the appropriate value for these experiments. The beam diameter at the corneal plane (103 cm from the output mirror) can then be calculated from the beam divergence and the $1/e^2$ beam diameter at 69 cm, giving a corneal spot size ($1/e^2$) of 1.47 mm.

EXPERIMENTAL PROCEDURES

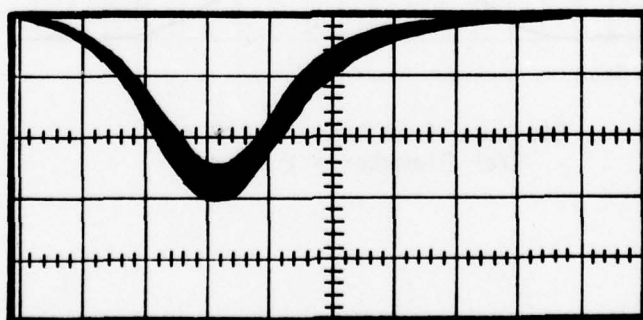
Each day before commencing a schedule of retinal exposures, the alignment of the movable mirror was checked and adjusted to assure that the reflected beam was coaxial with the fundus camera optic axis. Correct alignment was set by adjusting the mirror and, if necessary, the laser itself, so that the reflected beam spot projected on a Kodak IR phosphor screen coincided with the cross-hair



Time base: 100 nsec/division
Pulse-repetition rate: 0.1 kHz

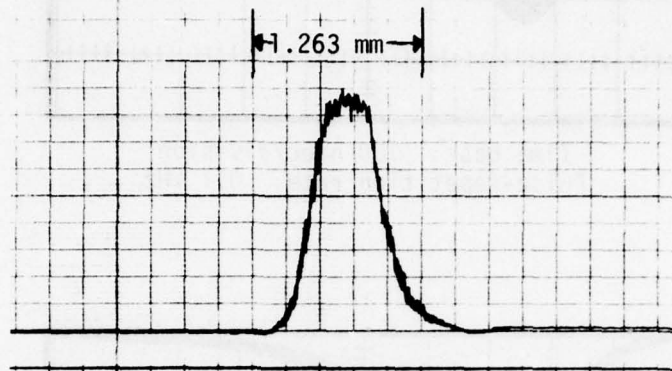


Time base: 100 nsec/division
Pulse-repetition rate: 1 kHz

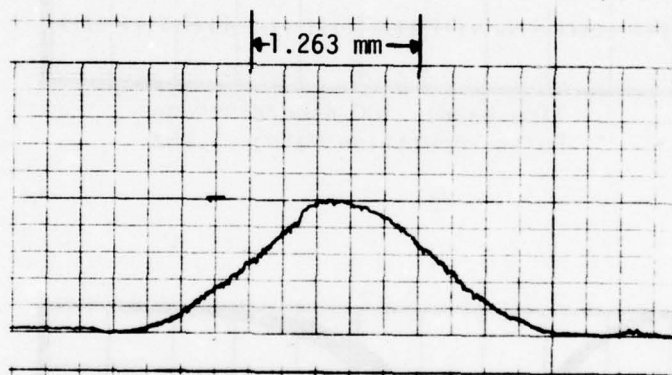


Time base: 200 nsec/division
Pulse-repetition rate: 10 kHz

Figure 3. Oscilloscope traces of repetitive, Q-switched Nd:YAG laser pulses.



Distance from Laser = 13.5 cm
 $1/e^2$ Diameter = 0.84 mm



Distance from Laser = 210 cm
 $1/e^2$ Diameter = 2.73 mm

Figure 4. Spatial intensity profiles of Nd:YAG laser beam in near (13.5 cm) and far (210 cm) fields.

intersection for two positions of the target, near the corneal plane and at a distance ~1.5 m from the camera. This procedure ensured that each exposure was precisely placed on a given macular site as selected by the cross-hairs. In addition, the beam was visually checked for radial symmetry by diverging it through a negative lens to a large spot size (several cm diameter) and projecting it on a Kodak IR phosphor screen.

Prior to exposure each primate subject was prepared as described in the Primate Care section and then refracted in each eye to determine the corrective lenses required. During the eye-exposure sequence, the eyelid was held open with a stainless steel speculum and the cornea was irrigated frequently with normal saline to maintain optical clarity.

Eight marker lesions, four arranged vertically and four horizontally, were placed adjacent to the macula to define the coordinate positions for the 16 test exposures within the macula, as shown in Figure 5. The 16 exposure intensities (peak pulse power) to be used were determined as follows. Based on previous experiments or on trial exposures of one or two animals, a preliminary ED50 was estimated for each exposure condition. Then 16 power levels, spaced uniformly on a log dose scale, were tabulated such that the estimated value was half-way down the scale and twice this power was at the top. This normally yielded a range in which the maximum power was about 3.7 times the minimum. The 16 exposures were delivered to the eye in a random sequence, with a different randomization for each eye. The sequence was unknown to the eye examiner so that his lesion evaluations would be unbiased.

Immediately prior to exposure, standard retinoscopy was performed on each eye to find the refractive error in white light. This value was increased by +0.5 diopter to allow for chromatic error introduced by 1064-nm light. If the dioptric error was greater than ± 0.5 , a corrective lens was interposed in the laser beam, in which case an additional correction was applied to compensate for the distance (10.2 cm) between the corrective lens and the eye. This was computed from the relation $F_y = F/(1 + D_y F)$, where F_y is the corrected power for the lens distance (D_y) measured from a plane 1.5 cm in front of the cornea (i.e., $D_y = 10.2 - 1.5$ cm), and F is the lens power uncorrected for distance. This distance correction was very small, and for most eyes, was generally less than 0.25 diopter.

In experiments where a corrective lens was required, its transmittance was measured in the laser beam in the CW mode. The transmittance was taken to be the ratio of beam power (as measured by the photodiode) with the lens in place to that without the lens, averaged over a set of 10-15 readings. The exposure energies as determined from the photographs of the oscilloscope traces were corrected by the transmittance factor. Transmission values for all lenses used were found to cluster around 92%.

The average peak power of a given exposure pulse was preset by adjusting the circular ND wedge while monitoring several test pulse traces on the oscilloscope (Fig. 1). The time that each exposure was made was recorded to the nearest minute. A photograph of each pulse trace was labeled with the exposure number and the oscilloscope scale settings for subsequent computation of laser power and pulsewidth. The designated retinal sites were then examined ophthalmoscopically one hour post-exposure using a simple lesion/no-lesion evaluation. In other words, no attempt was made to quantify retinal damage severity for the

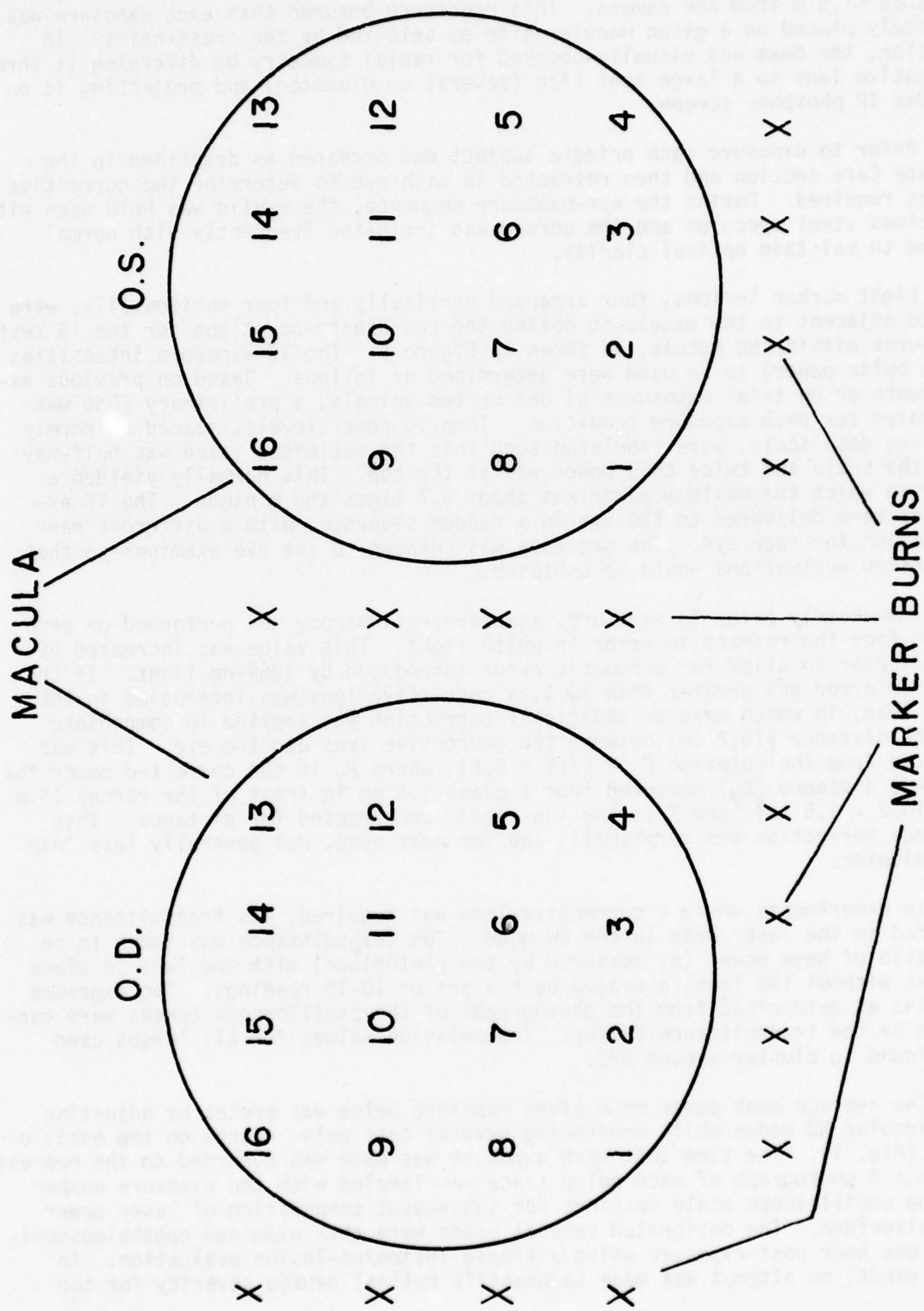


Figure 5. Diagram of macular exposure sites on rhesus retina.

purpose of statistical analysis. Preliminary ED50 thresholds were calculated on a Wang 700B programmable calculator using the method of probits. Tabular data on each subject eye were submitted to USAFSAM, Biometrics Division for final statistical analysis, as discussed in the Appendix. The latter values are reported here.

Normally, thresholds were calculated from observations of at least ten eyes. In some cases, more eyes were exposed and examined, especially if initial results showed wide variability or were otherwise questionable. In two cases, fewer than ten eyes were used, principally because of equipment failure and time limitations on the total program. These cases, as noted in the Results section, introduced negligible if any discrepancies.

RESULTS

ED50 thresholds were determined for 1064-nm laser radiation using the combinations of pulsewidth, repetition frequency and pulse-train duration listed in Tables 1 and 2. More than 280 rhesus eyes were used in this study.

Single-pulse threshold data obtained in this study are listed in Table 1 together with thresholds obtained by Skeen, et al. (24). These same data are displayed in Figure 6 as $\log(\text{ED50})$ vs. $\log(\text{pulsewidth})$. Also included in Table 1 are estimated thresholds for single-pulse 0.05-sec exposures and the effective CW limits for 2- and 5-pulse configurations of ≈ 300 nsec pulses, obtained from the solid curve in Figure 6. These interpolated values will be used in the discussion of multiple-pulse exposures. The data, thus displayed, show a relatively smooth, monotonic progression for pulsewidths ranging from ≈ 300 nsec to 120 sec, although there is a glaring paucity of experimental data in the range from ≈ 1 μsec to ≈ 1 msec. This trend could be anticipated on the basis of essentially thermal damage mechanisms; indeed, IITRI (44) thermal model calculations, assuming a retinal image radius (RIM) of 50 μm , show a distinctly similar trend as indicated in Figure 6. The solid curve represents the empirical relationship (45):

$$\text{ED50(mW)} = 48.64t^{-.1317} + 0.3492t^{-1} \quad (1)$$

for $t \geq 10^{-3}$ where t is exposure time (pulse width) in seconds. For $t < 10^{-5}$, a constant energy of 26.5 μJ is used. This is the mean of the two observed data points in this region.

Threshold data for repetitive, Q-switched 1064-nm pulses are summarized in Table 2 along with the corresponding pulse conditions and other statistical parameters of interest. We calculated preliminary ED50 values by two alternate probit methods. One involves a combined probit of exposure data from all test eyes taken collectively; the other involves separate probits of the data from each test eye, taken separately and then averaged to provide the ED50 value. Good agreement was obtained using the two methods. However, only the values obtained by USAFSAM, Biometrics Division, using the latter method, are reported here.

The entire data set is displayed in Figure 7 as a log-log plot of ED50 as a function of pulse repetition rate. In addition, the single-pulse threshold (107 W at 270 nsec) is included as the limiting, low-frequency terminal point, the frequency of which is taken, for convenience, as the reciprocal of each

TABLE 1. SINGLE-PULSE RETINAL DAMAGE THRESHOLDS AT 1060 nm

Pulsewidth	ED50 on cornea		90% Confidence interval ^a	No. of eyes	Notes
	Peak pulse power	Energy per pulse			
0.27 μ s	107 W	29.0 μ J	99 - 117 W	10	b
0.60	44.2	26.5	-	-	c
0.70	34.7	24.3	32.6 - 36.9	30	d
1.50	17.7	26.5	-	-	c
1 ms	443 mW	0.443 mJ	423 - 465 mW	30	d
10	146	1.46	140 - 153	28	d
50	79.2	3.96	67.2 - 93.2	-	c
100	67.3	6.72	63.1 - 71.7	31	d
500	53.0	26.5	50.9 - 55.1	12	b
1 sec	41.9 mW	41.9 mJ	38.4 - 45.8	32	d
5	40.9	205	38.6 - 43.3	21	b
30	31.1	933	26.1 - 37.0	-	c
120	27.6	3.31 μ J	25.0 - 30.4	9	e

^aMethods of calculating confidence intervals given in Appendix A for experimental and predicted estimates.

^bThis work.

^c0.6- and 1.5- μ sec estimates are interpolated, assuming constant energy of 26.5 μ J--all others indicated are calculated from equation (1), p. 19.

^dThresholds are from SAM analysis of original data (Ref. 24.)

^eReference (34).

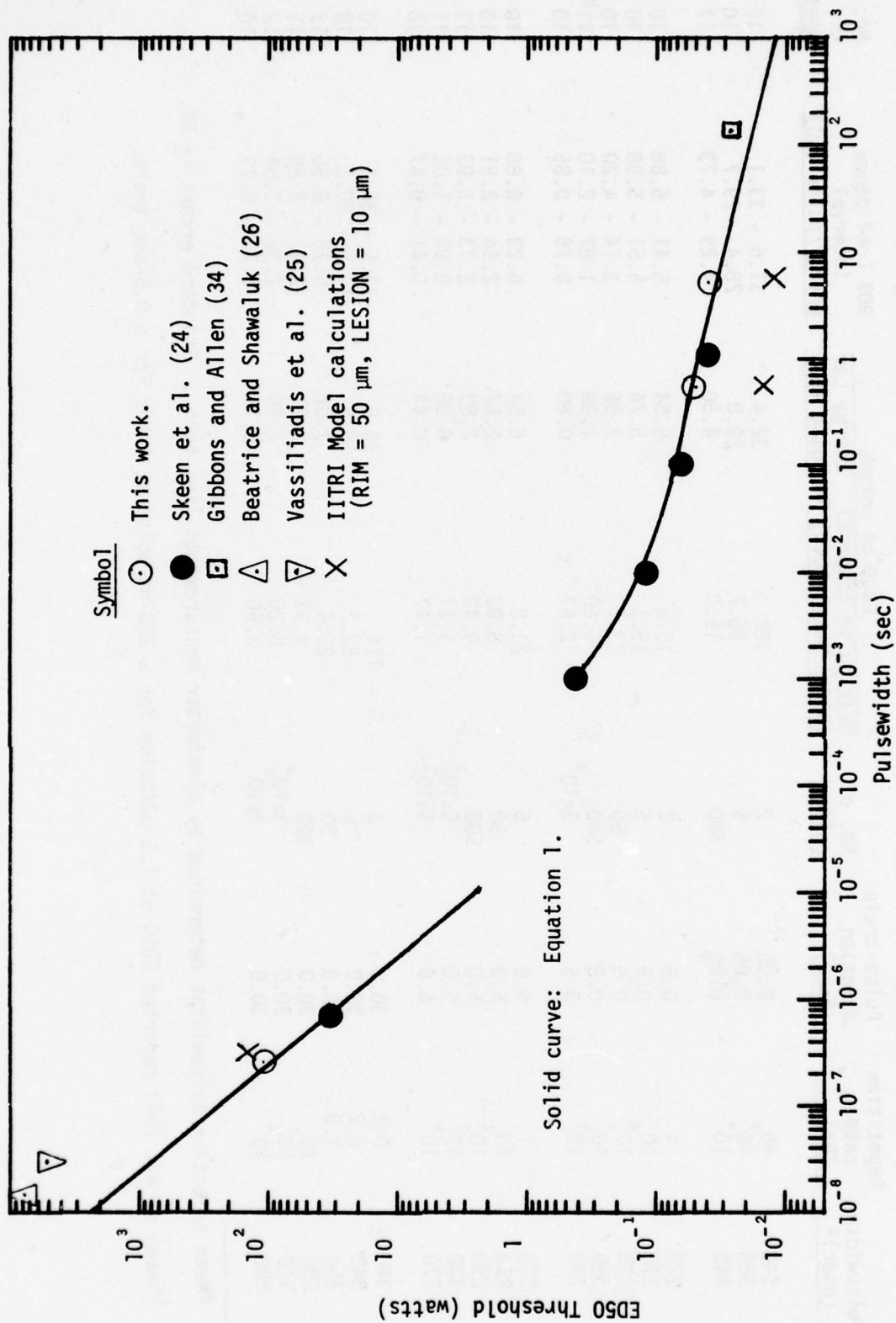


Figure 6. Experimental single-pulse retinal thresholds for Nd:YAG laser exposures (1064 nm).

TABLE 2. SUMMARY OF ED50 THRESHOLDS FOR RHESUS MACULAE EXPOSED TO REPETITIVE, Q-SWITCHED 1064-nm LASER PULSES

Pulsewidth (nsec) ^a	Repetition rate (Hz)	Pulse-train duration (sec)	No. of pulses	ED50 on cornea		90% Confidence interval energy/pulse (μJ)	No. of eyes
				Peak pulse power(W) (300ns pulsewidth)	Energy per pulse (μJ)		
340	40 ²	0.05	2	108	32.4	31.6 - 33.1	10
355	10 ⁴	0.05	5	96.7	29.0	28.4 - 29.7	10
840	10 ⁴	0.05	500	15.0	4.50	4.29 - 4.73	11
270	4	0.5	2	18.8	5.64	5.41 - 5.88	10
270	10 ²	0.5	5	19.1	5.74	5.51 - 5.98	10
270	10 ³	0.5	50	13.2	3.96	3.74 - 4.20	10
300	10 ⁴	0.5	500	6.60	1.98	1.87 - 2.10	11 ^b
730	10 ⁴	0.5	5x10 ³	2.67	0.80	0.75 - 0.85	10
270	1	5.0	5	21.8	6.54	6.23 - 6.88	10
290	10 ²	5.0	50	8.90	2.67	2.54 - 2.81	10
290	10 ³	5.0	500	9.43	2.83	2.73 - 2.93	11
300	10 ³	5.0	5x10 ³	3.27	0.98	0.91 - 1.06	11
770	10 ⁴	5.0	5x10 ⁴	1.47	0.44	0.41 - 0.47	10
340	0.1	30.0	3	116	34.8	33.5 - 36.1	10
340	0.2	30.0	6	62.7	18.8	17.5 - 20.2	10
350	1.0	30.0	30	23.4	7.02	5.76 - 8.56	12
280	10 ²	30.0	300	8.37	2.51	2.42 - 2.60	11
310	10 ³	30.0	3x10 ³	8.20	2.46	2.38 - 2.54	12
280	10 ⁴	30.0	3x10 ⁴	2.50	0.75	0.70 - 0.79	10

^aMean effective pulsewidths determined by planimeter measurements (see text). Standard errors = ± 8%.

^bSkeen et al. (24) reported ED50 of 1.5 μJ/pulse for a 700-ns pulse at 1 kHz for a 0.5-sec train.

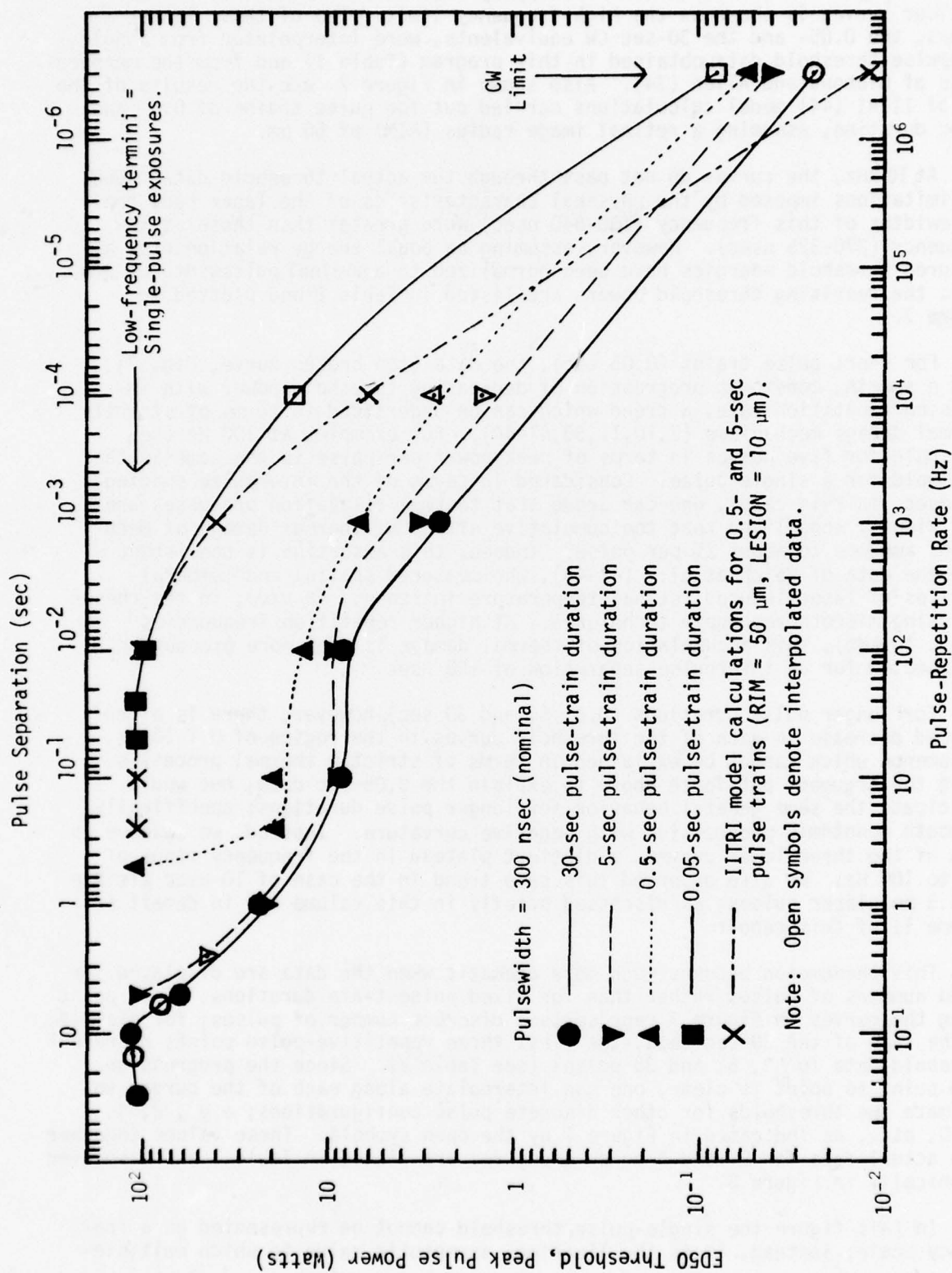


Figure 7. Summary of retinal threshold data for repetitive Q-switched Nd:YAG laser pulses (1064 nm).

respective pulse-train duration. The appropriate CW equivalent for each of the four curves is shown as the high-frequency limit. Two of these latter values, the 0.05- and the 30-sec CW equivalents, were interpolated from single, longpulse threshold data obtained in this program (Table 1) and from the measurements of Gibbons and Allen (34). Also shown in Figure 7 are the results of one set of IITRI (44) model calculations carried out for pulse trains of 0.5- and 5-sec duration, assuming a retinal image radius (RIM) of 50 μm .

At 10 kHz, the curves do not pass through the actual threshold data. Due to limitations imposed by the physical characteristics of the laser rod, the pulsewidths of this frequency (730-840 nsec) were greater than those at low frequency (270-325 nsec). However, assuming an equal energy relationship, all measured threshold energies have been normalized to a nominal pulsewidth of 300 nsec; the resulting threshold powers are listed in Table 2 and plotted in Figure 7.

For short pulse trains (0.05 sec), the data (top broken curve, Fig. 7) show a smooth, monotonic progression of decreasing threshold power with increasing repetition rate, a trend which can be understood in terms of strictly thermal damage mechanisms (7,10,11,30,41-44). For example, at 100 Hz the threshold for five pulses in terms of peak power per pulse is the same as the threshold for a single pulse. Considered in terms of the interpulse spacing (10 msec, in this case), one can argue that thermal relaxation processes are sufficiently long lived that the cumulative effect of thermal damage of mechanisms amounts to about 2% per pulse. Indeed, this assertion is consistent with the data of Welch et al. (41-43), who measured spatial and temporal profiles of laser-induced retinal temperature increases, *in vivo*, in the rhesus eye using microthermocouple techniques. At higher repetition frequencies (e.g., 10 kHz), this accumulation of thermal damage is even more pronounced, as expected for an interpulse separation of 100 μsec .

For longer pulse durations (0.5, 5, and 30 sec), however, there is a pronounced decrease in each of the threshold curves in the region of 0.1-10 Hz, a phenomenon which cannot be explained in terms of strictly thermal processes. Using the argument put forth above to explain the 0.05-sec data, one would anticipate the same general behavior for longer pulse durations; specifically, a smooth monotonic progression with negative curvature. Instead, we observe in each of the three lower curves, a distinct plateau in the frequency range of ~ 10 to 100 Hz. We also observed this same trend in the case of 10- μsec visible (514.5 nm) laser pulses, as discussed briefly in this volume and in detail in Volume II of this report.

This phenomenon becomes much more dramatic when the data are displayed for fixed numbers of pulses rather than for fixed pulse-train durations. Each point along the curves in Figure 7 represents a discrete number of pulses; for example, in the case of the 30-sec data, the first three repetitive-pulse points represent threshold data for 3, 6, and 30 pulses (see Table 2). Since the progression from point to point is clear, one can interpolate along each of the curves to estimate the thresholds for other discrete pulse configurations; e.g., 2, 4, 5, 10, etc., as indicated in Figure 7 by the open symbols. These values together with actual data for 2- and 5-pulse exposures are listed in Table 3 and displayed graphically in Figure 8.

In this figure the single-pulse threshold cannot be represented on a frequency scale; instead, it is the limiting, asymptotic value to which multiple-

TABLE 3. MEASURED AND INTERPOLATED THRESHOLDS
FOR 2- AND 5-PULSE EXPOSURES AT VARIOUS
SEPARATIONS OF 300 nsec Nd:YAG PULSES

No. of pulses	Pulse separation	Repetitive rate (Hz)	ED50 on cornea	
			Peak pulse power (Watts) ^a	Energy per pulse
2	$\rightarrow\infty$	$\rightarrow 0$	96.7 ^a	29.0
	15 sec	0.067	112 ^b	33.6
	2.5 sec	0.4	50 ^b	15.0
	0.25 sec	4	18.8	5.64
	0.025 sec	40	108	32.4
	0	3.3×10^6	43 ^c	12.9
5	$\rightarrow\infty$	$\rightarrow 0$	96.7 ^a	29.0
	6 sec	0.167	72 ^b	21.6
	1 sec	1	21.8	6.54
	0.1 sec	10	19.1	5.74
	0.01 sec	100	96.7	29.0
	0	$\approx 3.3 \times 10^6$	17 ^c	5.1

^aSingle-pulse datum, normalized to 300-nsec pulsewidth

^bInterpolated from curves of Figure 7.

^cCW limits interpolated from single-pulse data (Table 1).

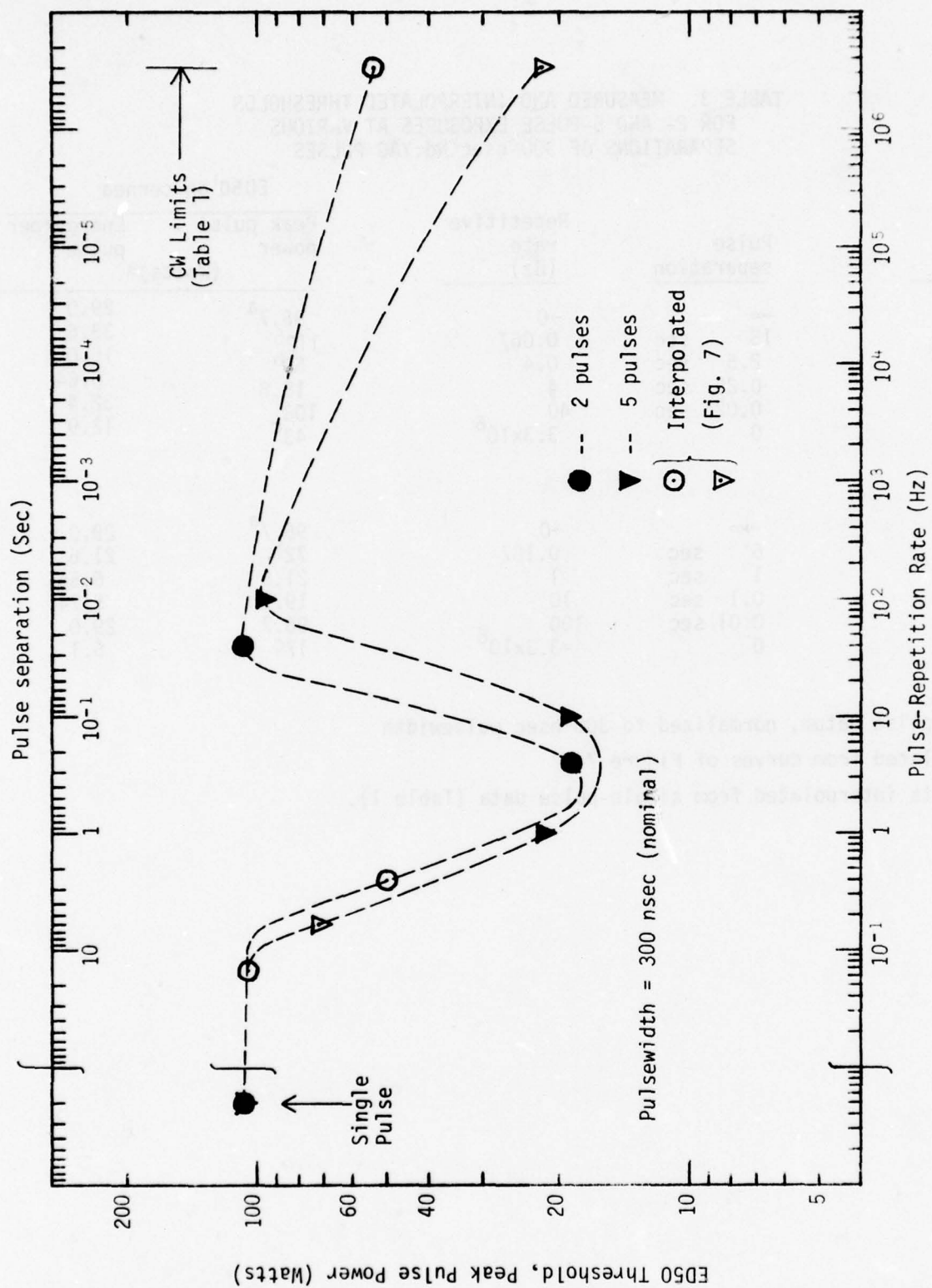


Figure 8. Retinal threshold vs. pulse separation for fixed numbers of Q-switched Nd:YAG laser pulses.

pulse thresholds converge in the limit as the interpulse spacing becomes much greater than ~ 10 sec. The high-frequency terminal points (i.e., CW limits), however, can be represented by the reciprocal of the nominal pulse duration (3.33 MHz). The threshold values for these two cases can be interpolated from the single-pulse data shown in Figure 6 for ~ 600 nsec and ~ 1.5 μ sec, respectively, for two and five pulses of 300-nsec pulsewidth.

As seen in Figure 8, repetitive Q-switched pulses of near-IR laser radiation constitute a more severe retinal hazard than do single pulses, especially when the interpulse spacing is between ~ 0.1 and 1 sec. Until additional threshold data are obtained, the optimum interpulse spacing and the depths of the minima can only be estimated. Nevertheless, two 300-nsec pulses delivered to the same site within ~ 0.5 sec are clearly more effective, by at least a factor of 5, than is a single pulse in causing irreversible, retinal damage. Moreover, the trends indicated in Figures 7 and 8 show that this factor must be considered as a lower limit; further experiments might well yield lower thresholds for other pulse configurations. The actual threshold for two Nd:YAG pulses at optimum spacing could be as low as $\sim 8W$. This is the plateau value for 30-sec pulse trains at ~ 10 Hz (Fig. 7 and Table 2), and probably constitutes a lower limit.

In any case, if a given laser at fixed pulsewidth can present ocular hazards that differ by a factor of ~ 10 , more research is urgently needed, not only to define the empirical hazard levels but also to gain a more fundamental understanding of the nature and variety of laser-induced retinal damage mechanisms.

The trend shown in Figure 8 for repetitive 300-nsec pulses at 1064 nm is strikingly similar to results obtained in this program for repetitive 10- μ sec pulses at 514.5 nm. In neither case can the obvious cumulative effect of retinal exposures be explained in terms of thermal damage mechanisms, at least at our present level of understanding of thermal effects of retinal tissues. Instead, one is forced to consider alternative damage mechanisms, chief among which is the possible involvement of photochemical and/or photobiological processes. These are discussed briefly in the following section and in some detail in Volume II of this report.

DISCUSSION

General Observations

We observed marked differences in the size, appearance and post-exposure time of occurrence between the lesions produced by CW single pulses and those produced by Q-switched repetitive pulses. The single-pulse lesions were relatively large in diameter and diffuse in appearance, whereas the Q-switched repetitive-pulse lesions were much smaller, more sharply defined, and appeared to be deeper. For the single-pulse exposures, the lowest energy lesions in all cases had considerably larger diameters than the lowest energy burns from Q-switched pulse trains. In reading the eye one hour after a single-pulse exposure, one could observe a set of large diameter lesions at sites exposed to the high energy pulses, but in some cases there was no evidence of damage at the sites exposed to the lower energy pulses. The eyes exposed to single-pulse radiation, therefore, exhibited a very distinct energy transition from "lesion" to "no lesion". Also, in single-pulse experiments, the two or three highest energy pulses always produced lesions that were clearly observable immediately after exposure.

On the basis of these observations, a distinct difference appears to exist between the nature of chorioretinal damage produced by long, CW pulses and that induced by repetitive, Q-switched pulses of 1064-nm radiation. These differences may reflect mechanism: in the case of long (≥ 0.05 sec), single-pulse exposures, strictly thermal processes appear to predominate; whereas in the case of Q-switched pulses, acoustic shock (46) may induce membrane disruption at power levels lower than required to initiate thermal damage. It is also conceivable that at the high corneal power densities required for near-IR-induced retinal damage ($\geq 10^4$ W/cm²), frequency doubling of the laser's fundamental output to 532 nm may occur within the anterior media (e.g., stroma or lens). If this were true, then photobiological processes induced in the retina by repetitive, visible pulses cannot be ruled out. This aspect is discussed in greater detail below.

Most eyes exposed to the Nd:YAG laser, both in the CW and Q-switched modes, showed a definite tendency to progress from a relatively clear state before exposure to a cloudy or diffuse state one hour after exposure. This condition made some retinal examinations very difficult, since the incident beam is directed through the center of the pupil for all 16 exposures in a given eye, and normally the post-exposure observations are also made through the center of the pupil. However, due to the radiation-induced clouding (47) of the anterior media along this direction, it was extremely difficult--in many cases impossible--to obtain a sharp view of the fundus. For this reason, the visual examinations of the fundus were performed by siting along a line through the upper periphery of the pupil. This provided a somewhat clearer view in most eyes, but in some eyes the fundus was impossible to see clearly along any viewing axis. Of the total eyes exposed to the YAG laser radiation, about 15% had to be discarded for purposes of threshold determinations, either because the eye was impossible to read or because the information obtained was totally inconsistent with the preponderance of data gathered under the same or similar circumstances.

The repetitive-pulse data indicate a critical need for further refinement of theoretical models to account for the decidedly anomalous behavior of threshold pulse power as a function of repetition rate, for argon-ion as well as Nd:YAG laser exposures. As discussed below, we hypothesize that photochemical and/or photobiological processes are involved in producing retinal threshold damage for certain repetitive-pulse conditions.

In cases where damage is induced by repetitive, visible laser pulses of pulsewidth ≥ 100 μ sec, we find generally good agreement between experimental results and theoretical calculations predicted exclusively on thermal damage mechanisms. This indicates that thermal processes (high temperature gradients), possibly unaided by any concurrent photochemical processes, are chiefly responsible for producing damage (e.g., through the mechanisms of protein denaturation or enzyme inactivation (3)).

However, in the case of threshold damage induced by repetitive visible pulses of shorter pulsewidths and higher intensities, especially pulses shorter than 10 μ sec, we find serious disparities between experiment and theory. Considered in terms of double-pulse exposures, we hypothesize that even if the energy of the initial pulse is insufficient to induce thermal damage, its intensity (power) may reach a level sufficient to trigger a photochemical reaction, possibly involving one or more intermediate stages of the photopigment cycle;

e.g., production of excess opsin in the receptors, accumulation of excess retinol in the pigment epithelium, or production of high localized Na^+ or Ca^{++} concentrations in the outer segments (48). Whatever the initial reaction or its products, the cumulative effects appear to be maximal within a few seconds after photic stimulation (Fig. 8), the result being a significantly greater susceptibility to damage, whether by photochemical or by thermal effects. Thus, a second pulse arriving within this time interval requires less energy to induce damage than if it were to arrive either well before or well after the maximum effect of the initial pulse.

For visible laser radiation (Volume II), this rather general approach adequately accounts for the observed minima in the double-pulse thresholds as a function of pulse separation. It also accounts for the minima observed with 3-, 5-, and 10-pulse exposures (49). In the latter cases, each pulse after the first presumably induces damage of the products of the reaction triggered by the preceding pulse, and also retriggers this same reaction to provide additional products which, in turn, can be damaged by succeeding pulses.

As discussed in detail in Volume II of this report, a two-mechanism/two-threshold hypothesis offers an attractive explanation of the results of visible laser pulses. However, such an hypothesis presents obvious difficulties if applied to the strikingly similar results obtained using near-IR (1064 nm) laser radiation. Photochemical damage mechanisms at this wavelength would appear to be highly implausible unless intermediate processes, such as two-photon absorption or frequency doubling of the radiation, are also postulated. However, in view of the similarities in threshold behavior at both the visible and near IR-wavelengths, the latter mechanisms should not be ruled out entirely.

At least partial clarification may be achieved through comparative histological investigation of both types of threshold damage, i.e., damage induced by repetitive visible as well as near-IR laser pulses. Detailed comparison of microscopic appearances as well as the site of primary damage within the retina should reveal similarities or differences which would help identify the mechanisms involved in each type of exposure.

Thermal Model Calculations

As noted previously, the threshold data obtained for repetitive ~ 300 -nsec, near-IR pulses (Figs. 7 and 8) are remarkably similar to data obtained using 10- μ sec, visible (514.5 nm) pulses. For reference purposes, we include here the analogous data obtained using the argon-ion laser. Figure 9 displays all data obtained in this program for repetitive, 10- μ sec, 514.5-nm pulses for 0.05, 0.5, 5 and 30-sec pulse trains (analogous to Fig. 7) while Figure 10 shows the same data but plotted for fixed configurations of 2, 3, 5 and 10 pulses (analogous to Fig. 8). The similarity between the results obtained using two entirely different sets of laser parameters (wavelength, divergence, pulsewidth) suggests that we are observing the effects of similar mechanisms in both cases. It is clear that both cases represent marked departures from strictly thermal behavior.

Table 4 lists peak temperatures predicted by the IITRI thermal model (44) for output powers representative in single- and multiple-pulse thresholds for both 10- μ sec visible and ~ 300 -nsec near-IR laser pulses. Two conclusions can be drawn from these results. First, realistic temperature calculations require

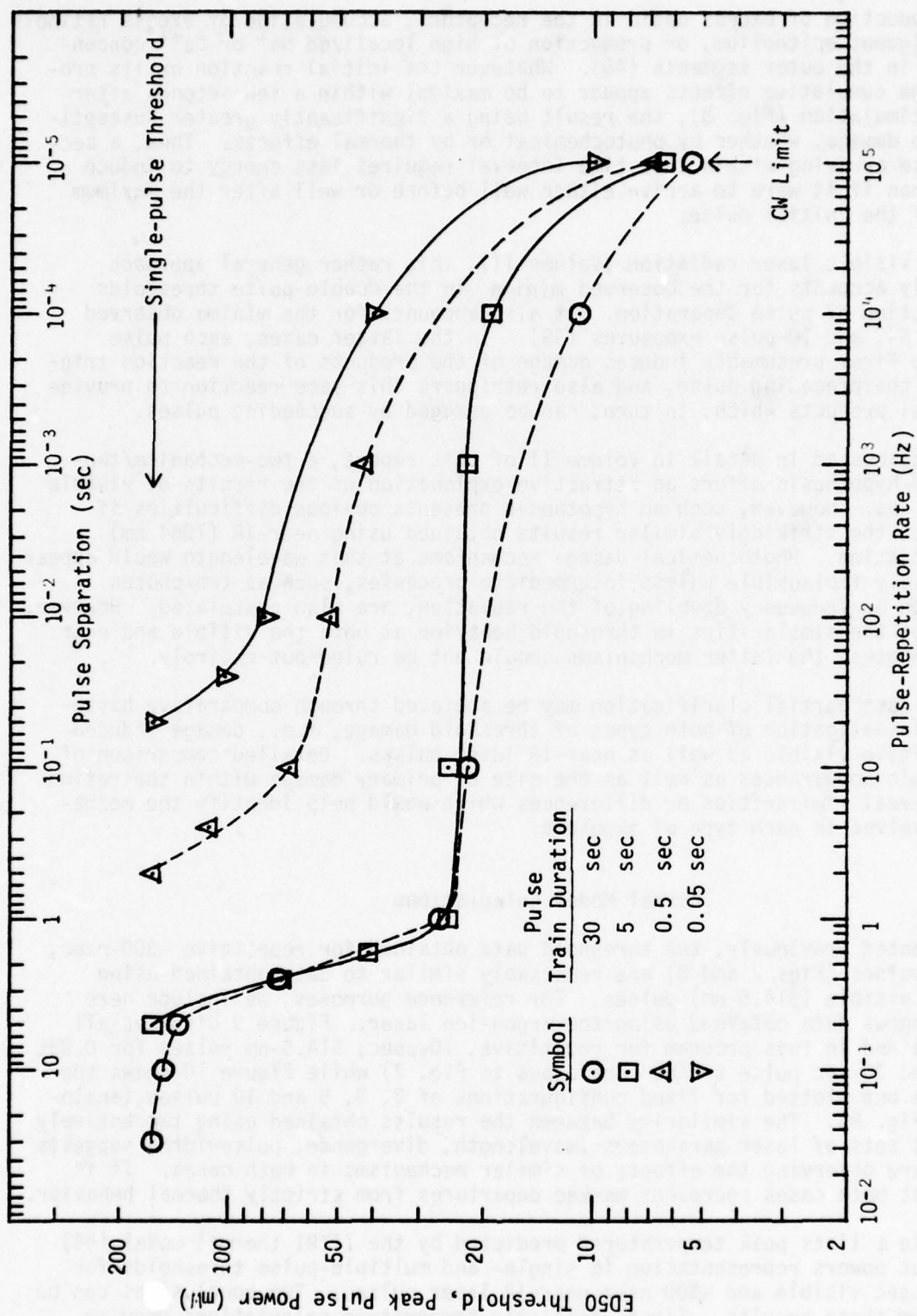


Figure 9. Observed retinal thresholds vs. repetition rate for 0.05-30-sec trains of 10- μ sec, 514.5-nm laser pulses.

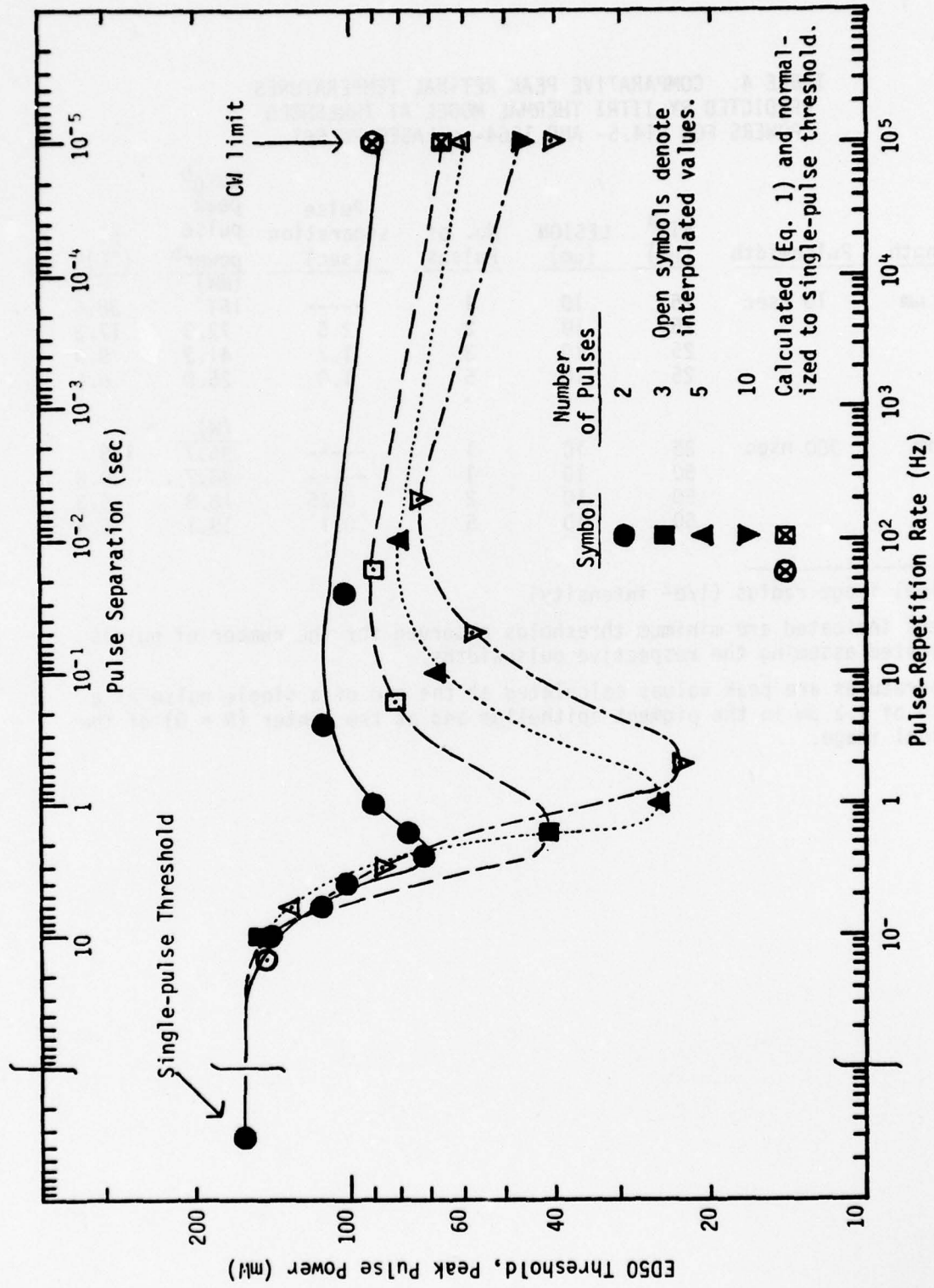


Figure 10. Retinal threshold vs. pulse separation for fixed numbers of repetitive 10- μ sec, 514.5-nm laser pulses.

TABLE 4. COMPARATIVE PEAK RETINAL TEMPERATURES
PREDICTED BY IITRI THERMAL MODEL AT THRESHOLD
POWERS FOR 514.5- AND 1064-nm LASER PULSES

Wavelength	Pulsewidth	RIM ^a (μ m)	LESION (μ m)	No. of Pulses	Pulse separation (sec)	ED ₅₀ ^b peak pulse power ^b (mW)	ΔT (°C) ^c
514.5 nm	10 μ sec	25	10	1	-----	161	38.6
		25	10	2	2.5	72.3	17.3
		25	10	3	1.7	41.3	9.9
		25	10	5	1.0	25.0	6.0
1064 nm	300 nsec	25	10	1	-----	(W) 96.7	190
		50	10	1	-----	96.7	30.0
		50	10	2	0.25	18.8	5.3
		50	10	5	0.1	19.1	5.4

^a Retinal image radius ($1/e^2$ intensity)

^b Powers indicated are minimum thresholds observed for the number of pulses indicated assuming the respective pulsewidths.

^c Temperatures are peak values calculated at the end of a single pulse at a depth of 1.2 μ m in the pigment epithelium and at the center ($R = 0$) of the retinal image.

accurate experimental measurements of retinal image sizes. The respective values of the RIM parameter chosen for these calculations, 25 and 50 μm , are considerably larger than retinal image radii calculated by ray-trace techniques (50), although the ratio is approximately correct for beam divergence angles of 0.6 mrad (514.5 nm) and 1.2 mrad (1064 nm). However, smaller retinal spot sizes will yield even higher, and probably unrealistic, calculated temperatures, as shown in Table 4 by the comparative values for 1064-nm laser pulses.

Second, the 514.5-nm calculations show clearly that strictly thermal damage mechanisms cannot account for the multiple-pulse thresholds, even if one assumes that the single-pulse threshold (161 mW) is representative of such mechanisms. Thus, if a peak temperature increase of $\sim 38^\circ\text{C}$ is required to induce thermal damage, then irreversible damage would not be anticipated at the proportionately lower temperatures predicted for the laser powers observed for minimum repetitive-pulse thresholds.

In this connection, it must be borne in mind that thermal relaxation processes in retinal tissues are very fast relative to the optimal interpulse spacings (1-2 sec) shown in Figures 8 and 10. For example, IITRI model calculations indicate that a peak temperature increase of $\sim 17^\circ\text{C}$ (representative of a single, 70-mW, 10- μsec , 514.5-nm laser pulse) will subside to less than 2°C within ~ 0.5 msec after the end of the pulse. This may be compared with the microthermocouple measurements of Welch and co-workers (41-43) who observed thermal relaxation times (1/e) of ~ 100 msec following 10-msec, sub-threshold exposures of much larger retinal areas (≥ 150 μm radius).

Working Hypotheses to Explain Cumulative Effects of Repetitive Laser Pulses

Since purely thermal mechanisms cannot explain the repetitive-pulse experimental threshold data (Figs. 8 and 10), we are compelled to invoke other processes. The most likely alternative appears to be involvement of photochemical or photobiological damage mechanisms, although contributions of thermal effects are not necessarily excluded.

For the moment, we shall consider only the threshold data for visible wavelengths (Figs. 9 and 10). Departures from apparent thermal behavior do not become distinct until the pulse duration is decreased well below 1 msec (see Volume II). Thus, for 100- and 40- μsec pulses, slight departures from predicted thermal behavior are observed but the effect does not become pronounced until 10- μsec laser pulses are used. This suggests that the minima in Figure 10, and by extension in Figure 8 as well, represent an intensity- rather than an energy-dependent phenomenon.

This is borne out by threshold data for widely disparate pulsewidths of 1 msec and 10 μsec . At a pulse separation of 1 sec, the threshold (in terms of peak power per pulse) for five, 1-msec pulses is ~ 20 mW; for five, 10- μsec pulses at the same separation, the threshold is ~ 25 mW. Thus, in the case of 1-msec pulses, the energy per pulse at threshold is nearly 100-fold greater than for 10- μsec pulses, but the intensity (Watts \propto photons/sec) is about the same. For a single, 1-msec pulse the threshold (21 mW) is within experimental error of the five-pulse threshold, indicating no additivity of effects for consecutive, 1-msec pulses. In contrast, the threshold for a single, 10- μsec pulse (161 mW) is some 6.4 times higher than for five pulses, a factor which indicates the magnitude of additive effects of optimally separated 10- μsec visible laser pulses.

We suggest in Volume II a set of working hypotheses against which to test future experiments directed towards studies of the retinal damage mechanisms involved here. Briefly, in the case of double-pulse configurations, the primary effect (or influence) of each pulse may be either thermal or photochemical. However, based on the considerations discussed above, we tend to rule out thermal effects of the initial pulses. Hence we are left with two alternative working hypotheses.

In both cases, we consider that the effect of the first pulse involves quantum conversion of the incident laser pulse; whether this involves photochemical processes (i.e., relatively rapid molecular changes due to chemical reactions of excited electronic states) or photobiological processes (e.g., alteration, possibly longer term, of biological activity) remains to be determined. In either case, it is apparent that the effect of the first pulse is reversible: a single pulse does not by itself induce observable damage at the minimum threshold power for double pulses (~ 20 W for 1064-nm radiation).

The effect of the second pulse may be either thermal or photic. In the former instance, we suggest (Volume II) that thermal denaturation of free opsin, the protein moiety of the visual pigment rhodopsin, may be involved in the damage mechanism. Light intensities typical of those used in these experiments induce high concentrations (51-53) of this protein, which has been shown to be more thermally labile when in the free state (4) than when bound either to the chromophore or to outer-segment membranes. Moreover, *in vivo* thermal denaturation of free opsin has been implicated in electron microscope studies of light-induced retinal dystrophy in rats (4-6, 54) under conditions such that retinal temperature increases were as low as 3°C .

The alternative hypothesis invokes photic effects for both pulses. As suggested in Figure 8, at the optimum spacing for both two and five near-IR pulses (~ 0.2 - 0.5 sec), the minimum threshold is in the neighborhood of ~ 20 W per pulse. This appears to be a "saturating" value, so to speak, since even for ten pulses, the threshold does not appear to change significantly (Fig. 7). In other words, whatever damage is observed after ten pulses was induced by the first two to five pulses. Accordingly, the effect of the first pulse can be considered to be a reversible photo-trigger, for which the threshold power is about 20 W (at the cornea). If the effect of subsequent pulses is primarily photochemical, the reciprocity relationship should hold; i.e., the effects of subsequent pulses should depend more on the total energy of these pulses than on the peak power per pulse. The data listed in Table 5 show that this appears to be the case for the visible (514.5 nm), but there are insufficient data in the near-IR region to make a comparison.

The two working hypotheses may be abbreviated as photo + thermal (A) and photo + photo (B). Double-pulse experiments at 1064 nm should be undertaken to test these two general mechanisms. One such experiment would involve independent variation of the power levels of the two pulses; the results should provide a clear preference between these two alternatives. Specifically, hypothesis A predicts that the concentration of free opsin (or other thermally labile species) will be proportional to the intensity of the initial pulse (at least up to a saturating value). Since the effect of the second pulse is considered to be essentially thermal, only the temperature change induced by that pulse *in the labile molecules* is important. We assume a normal (i.e., Boltzmann) distribution of temperatures among the molecules in the irradiated

TABLE 5. THRESHOLD POWERS AND ENERGIES FOR
 REPETITIVE, 10- μ SEC, 514.5-nm
 LASER PULSES AT OPTIMUM SPACING
 ED50 on cornea

No. of Pulses (N)	Pulse separation (sec)	Peak pulse (mW)	Energy per pulse (μ J)	Total energy N pulses (μ J)	Total energy N-1 pulses (μ J)
2	2.5	72	0.72	1.43	0.72
3	1.7	41	0.41	1.24	0.82
5	1.0	25	0.25	1.25	1.00
10	0.5	23	0.23	2.30	2.07

area and that a minimum number of labile molecules (e.g., opsin) must be denatured to induce an observable lesion within one hour after exposure. Thus, hypothesis A predicts a smoothly varying dependence of the threshold power of the second pulse (I_2) as a function of the intensity of the initial pulse (I_1). This is shown in Figure 11(A), which may be summarized as follows: the lower the concentration of free opsin (at low I_1) the higher the local temperature change required to damage the critical number of free opsin molecules in the irradiated volume element. Conversely, at high I_1 , higher concentrations of free opsin will be formed and thus lower peak temperatures will be required to damage the critical number of labile intermediates.

In contrast, hypothesis B predicts that the threshold power for both pulses will be ~ 20 W, as shown in Figure 11(B). Thus, for retinal damage to occur, this hypothesis requires that the intensity of both pulses be above the threshold. If either I_1 or I_2 is less than ~ 20 W, no damage will occur.

In addition to providing more quantifiable predictions, hypothesis B has the advantage of being more amenable than its alternate to experimental verification of predictions of other N-pulse ($N > 2$) configurations. However, both hypotheses can be tested under a variety of double-pulse conditions, such as variation of the width of the second pulse. For example, both hypotheses predict that a 20 W, 300-nsec pulse followed at optimum spacing by a sufficiently energetic pulse of any other duration should cause observable damage. A clear preference between the two mechanisms can be made on the basis of: A--constancy of observed (or calculated) retinal temperatures, or B--constancy of total energy of the second-pulse threshold.

Although the above discussion is much more straightforward in the case of 514.5-nm laser pulses, plausible mechanisms other than direct, single-photon absorption processes exist which permit us to consider the repetitive pulse, near IR retinal threshold data in parallel with data obtained using visible laser radiation. Doubling of the fundamental frequency of ruby laser pulses (694.3 nm) has been observed experimentally in excised corneal tissues, albeit at extremely low conversion efficiencies (55). This phenomenon almost certainly occurs in the stroma, behaving as a nonlinear crystal. It is conceivable that the lens could likewise behave as a nonlinear optical medium, possibly with higher doubling efficiencies than the cornea because of its greater thickness.

Efficiency of second harmonic generation (SHG) depends strongly upon both the power density and the mode purity of the incident laser beam. In the Nd:YAG experiments cited here, precautions are taken to assure that only the TEM_{00} mode is incident on the subject eye. Furthermore, the repetitive-pulse intensities for near-IR damage threshold are on the order of tens of watts as opposed to tens of milliwatts for visible wavelength thresholds.

On a more quantitative basis, the double-pulse threshold at 1064 nm is about 20 W at optimum spacing (~ 0.5 sec). This power, incident on a ~ 1.5 mm diameter corneal spot, yields a power density of $\sim 10^4$ W/cm², as compared with ~ 1 W/cm² for 25 mW of 514.5-nm radiation incident on a corneal spot of 1.8 mm. Thus, a frequency-doubling efficiency of less than 0.1% for 1064-nm radiation could give rise to the intensity of visible light required for the reversible photo-trigger invoked in the two hypotheses discussed above. The experiment thus suggested is quite straightforward.

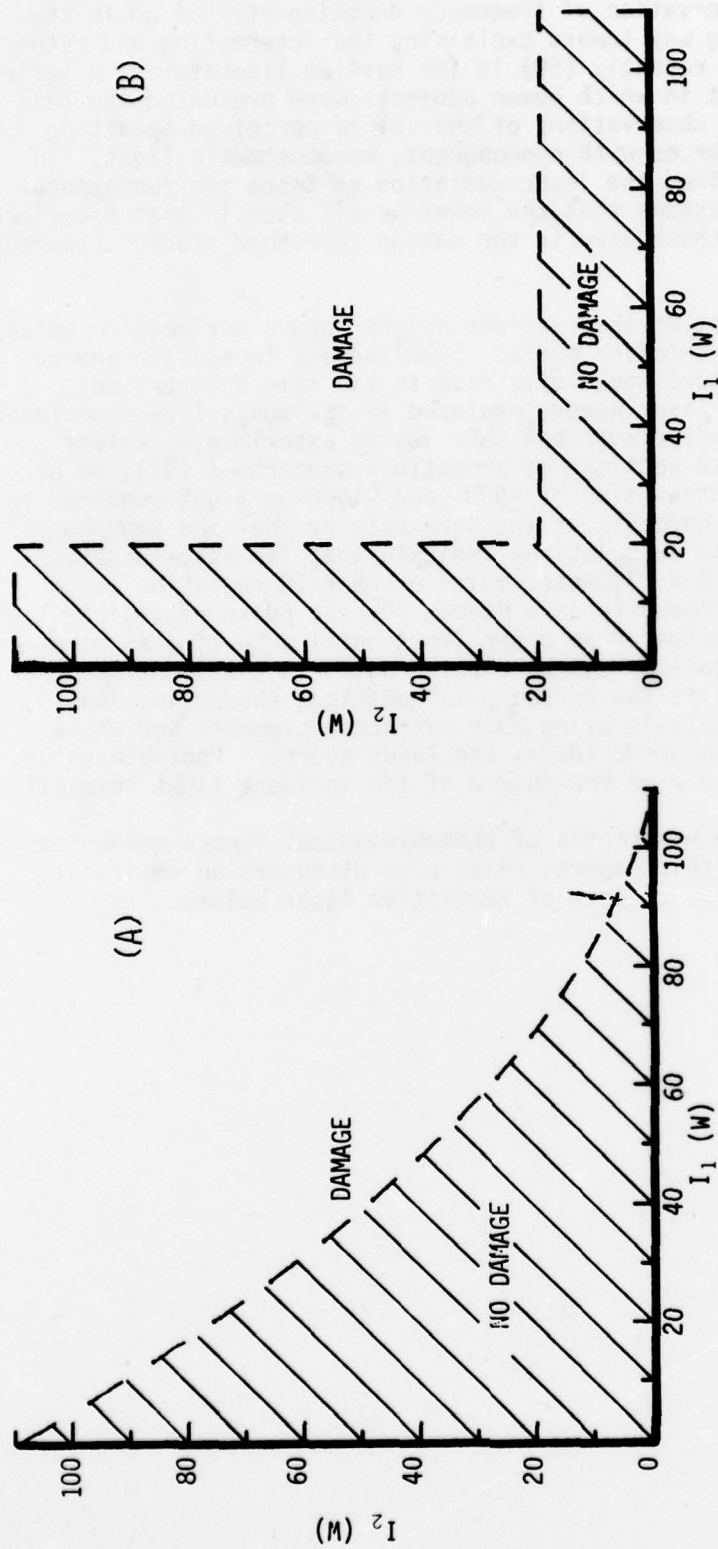


Figure 11. Idealized interpulse power dependencies predicted by working hypotheses for double-pulse threshold experiments. (A) The effects of the two pulses are assumed to be photic and thermal, respectively. Increasing concentrations of a thermally labile intermediate at higher initial pulse intensities (I_1) require lower peak temperatures induced by the second pulse (I_2). (B) The effects of both pulses are photic: the reversible trigger (I_1) requires a threshold of ~ 20 W after which the second pulse also has a threshold of ~ 20 W for irreversible photochemical damage. Both cases assume double 300-nsec, 1064-nm pulses separated by $\sim 0.2 - 0.5$ sec. (Adapted from Fig. 26, Vol. II of this report.)

In addition to its possible importance in explaining our repetitive-pulse Nd:YAG data, experimental observation of frequency doubling of 1064 nm in the anterior media would go a long way toward explaining the interesting and rather curious observations reported recently (56) in the Russian literature. A series of experiments was carried out in which human subjects were presented the task of comparing their subjective observations of the colors perceived emanating from various near-IR laser sources with noncoherent, monochromatic light. In all cases, the subjects perceived the laser radiation at twice the fundamental frequency. It seems safe to assume that the power levels used in that experiment were considerably lower than those used in the damage threshold studies reported here.

In any case, these subjective observations neither prove nor require actual SHG of laser radiation in the anterior media. Simultaneous two-photon absorption by the visual photoreceptors would give rise to the same observations. Moreover, considering the low laser powers employed in the subjective experiments, this mechanism could be more efficient than SHG. Using experimental values for two-photon absorption cross-sections of aromatic hydrocarbons (57), we have estimated (58) the relative intensities of ~ 500 - and ~ 1000 -nm light required to pump the $S_0 \rightarrow S_1$ transition of rhodopsin at the same rate by one- and two-photon processes, respectively. These calculations indicate that for assumed retinal image diameters of $\sim 25 \mu\text{m}$, a 20-W, 300-nsec pulse of near-IR radiation could be as effective in bleaching rhodopsin as a 25-mW, 10- μsec pulse of visible light. This estimate (58) must be considered an upper limit until such time as rigorous quantum mechanical calculations can be carried out. In the meantime, the experiment again suggests itself: the molecule in question, rhodopsin, should be studied by laser flash photolysis using both extracted pigments and whole disc preparations, and Nd:glass or Nd:YAG as the laser source. Photobleaching, if observed, will depend linearly on the square of the incident light intensity.

Further discussion of the hypothesis of photobiological damage mechanisms will be found in Volume II of this report, which also discusses an empirical model to describe the cumulative effects of repetitive laser pulses.

REFERENCES

1. Mainster, M. A., et al. Retinal temperature increases produced by intense light sources. *J Opt Soc Am* 60:264 (1970).
2. White, T. J., et al. Chorioretinal thermal behavior. *Bull Math Biophysics* 32:315 (1970).
3. Wood, T. H. Lethal effects of high and low temperatures on unicellular organisms. In *Advances in biological and medical physics*, Vol IV. New York: Academic Press, 1956.
4. Kuwabara, T., and R. A. Gorn. Retinal damage by visible light: An electron microscope study. *Arch Ophthalmol* 79:69 (1968).
5. Noell, W. K., et al. Retinal damage by light in rats. *Invest Ophthalmol* 5:450 (1966).
6. Friedman, E., and T. Kuwabara. The retinal pigment epithelium: IV - the damaging effects of radiant energy. *Arch Ophthalmol* 80:265 (1968).
7. Allen, R. G., et al. Research to obtain eye effects data and develop a mathematical model for eye effects predictions. Technology Incorporated, Contract F41609-70-C-0007, USAF School of Aerospace Medicine Final Report, Dec 1970.
8. Miller, N. D., and T. J. White. Retinal burns and flashblindness. Technology Incorporated, Contract F41609-68-C-0023, USAF School of Aerospace Medicine, Final Report, Vol. 1, Nov 1969.
9. Technology Incorporated. A study of retinal temperature predictions for high altitude weapon detonations. DASA Contract 01-09-C-0121, Quarterly Progress Report, Feb 1970.
10. Allen, R. G., et al. Research on ocular effects produced by thermal radiation. Technology Incorporated, Contract AF 41(609)-3099, USAF School of Aerospace Medicine, Final Report, July 1967.
11. Mainster, M. A., T. J. White and R. G. Allen. Spectral dependence of retinal damage produced by intense light sources. *J Opt Soc Am* 60:848 (1970).
12. Mainster, M. A. Destructive light adaptation. *Ann Ophthalmol* 2:44 (1970).
13. Sliney, D. H., et al. Laser hazards bibliography. U.S. Army Environmental Hygiene Agency, Aberdeen Proving Ground, Md., May 1975.
14. Dunskey, I. L., and P. W. Lappin. Evaluation of retinal thresholds for CW laser radiation. *Vision Res* 11:733 (1971).

15. Bresnick, G. H., et al. Ocular effects of argon laser radiation. *Invest Ophthalmol* 9:901 (1970).
16. Ham, W. T., et al. Helium-neon laser in the rhesus monkey. *Arch Ophthalmol* 84:798 (1970).
17. Frisch, G. D., E. S. Beatrice, and R. C. Holten. Comparative study of the argon and ruby retinal damage thresholds. *Invest Ophthalmol* 10:911 (1971).
18. Vassiliadis, A., H. C. Zweng and K. G. Dedrick. Ocular laser threshold investigations. Stanford Research Institute, Contract F41609-70-C-0002, USAF School of Aerospace Medicine, Final Report, Jan 1971.
19. Ebberts, R. W. Retinal effects from multiple pulse gallium arsenide lasers. SAM-TR-72-25, Nov 1972.
20. Skeen, C. H., et al. Ocular effects of repetitive laser pulses. Technology Incorporated, Contract F41609-71-C-0018, USAF School of Aerospace Medicine, Final Report, June 1972.
21. Fahs, J. H. A model for the study of retinal damage due to laser radiation. Technical Report 3678, Picatinny Arsenal, Feb 1968.
22. Hayes, J. R. and M. L. Wolbarsht. Thermal model for retinal damage induced by pulsed lasers. *Aerosp Med* 39:474 (1968).
23. Lappin, P. W. and P. S. Coogan. Relative sensitivity of various areas of the retina to laser radiation. *Arch Ophthalmol* 84:350 (1970).
24. Skeen, C. H., et al. Ocular effects of near infrared laser radiation for safety criteria. Technology Incorporated, Contract F41609-71-C-0016, USAF School of Aerospace Medicine, Final Report, June 1972.
25. Vassiliadis, A., R. C. Rosan and H. C. Zweng. Research on ocular laser thresholds. Stanford Research Institute, Contract F41609-68-C-0041, USAF School of Aerospace Medicine, Final Report, Aug 1969.
26. Beatrice, E. S. and P. D. Shawaluk. Q-switched neodymium laser retinal damage in rhesus monkey. Joint AMRDC-AMC Laser Safety Team, Memorandum Report M-73-9-1, Mar 1973.
27. Gibbons, W. D., and D. E. Egbert. Ocular damage thresholds for repetitive pulse laser exposures. SAM-TR-74-1, Feb 1974.
28. King, R. G. and W. J. Geeraets. The effect of Q-switched ruby laser on retinal pigment epithelium in vitro. *Acta Ophthalmol* 46:617 (1968).
29. Clarke, A. M. Ocular hazards. In R. J. Pressley (ed.). *Handbook of lasers with selected data on optical technology*. Cleveland: Chemical Rubber Publishing Company, 1971.
30. Sliney, D. H. The development of laser safety criteria--biological considerations. In M. L. Wolbarsht (ed.). *Laser applications in medicine and biology*, Vol. I. New York: Plenum Press, 1971.

31. Ebbers, R. W. and I. L. Dunskey. Retinal damage thresholds for multiple pulse lasers. *Aerosp Med* 44:317 (1973).
32. Adams, D. O., D. J. Lund and P. D. Shawaluk. The nature of chorioretinal lesions produced by the gallium arsenide laser. *Invest Ophthalmol* 13: 471 (1974).
33. Gibson, G. L. M. Retinal damage from repeated subthreshold exposures using a ruby laser photocoagulator. SAM-TR-70-59, Oct 1970.
34. Gibbons, W. D. and R. G. Allen. Evaluation of retinal damage produced by long-term exposure to laser radiation. SAM-TR-75-11, Apr 1975.
35. Boettner, E. A. and J. R. Wolter. Transmission of the ocular media. *Invest Ophthalmol* 1:776 (1962).
36. Boettner, E. A. Spectral transmission of the eye. University of Michigan, Contract AF Y1(609)-2996, USAF School of Aerospace Medicine, Final Report, July 1967.
37. Boettner, E. A. and D. Dankovic. Ocular absorption of laser radiation for calculating personnel hazards. University of Michigan, Contract F41609-74-C-0008, USAF School of Aerospace Medicine, Final Report, Oct 1974.
38. Coogan, P. S., W. G. Hughes and J. A. Mollsen. Histologic and spectrophotometric comparisons of the human and rhesus retina and pigmented ocular fundus. Chicago Presbyterian Hospital, Contract F41609-71-C-0006, USAF School of Aerospace Medicine, Final Report, Jan 1974.
39. Zuclich, J. A. and J. S. Connolly. Ocular hazards of ultraviolet laser radiation. In *Research on the ocular effects of laser radiation*. Technology Incorporated, Contract F41609-73-C-0017, USAF School of Aerospace Medicine, Second Annual Report Feb 1975.
40. Zuclich, J. A., and J. S. Connolly. Ocular damage induced by near-ultraviolet laser radiation. *Invest Ophthalmol* 15:760 (1976).
41. Welch, A. J., C. P. Cain and L. A. Priebe. Investigation of temperature rise in the fundus exposed to laser radiation. The University of Texas at Austin, Contract F41609-73-C-0031, USAF School of Aerospace Medicine, Final Report, May 1974.
42. Priebe, L. A., C. P. Cain and A. J. Welch. Temperature rise required for production of minimal lesions in the *Macaca mulatta* retina. *Am J Ophthalmol* 79:405 (1975).
43. Welch, A. J., et al. Limits of applicability of models of thermal injury. The University of Texas at Austin, Contract F41609-76-C-0005, USAF School of Aerospace Medicine, Interim Technical Report, May 1976.
44. Takata, A. N., et al. Thermal model of laser-induced eye damage. Illinois Institute of Technology Research Institute (IITRI), Contract F41609-74-C-0005, USAF School of Aerospace Medicine, Final Report, Oct 1974. (This report contains a comprehensive survey of the literature on thermal effects in biological systems as well as a review of earlier computer models of thermal injury.)

45. McNee, R. C., Prediction of a single pulse ED50. Unpublished Report, USAF School of Aerospace Medicine (SAM/BRD), May 1975.
46. Carome, E. G., et al. Generation of acoustic signals in liquids by ruby-induced thermal stress transients. *Appl Phys Lett* 4:95 (1964).
47. Miller, N. D. An experimental investigation of the effect of 1.06 μ m laser light on the transparent ocular media. Technology Incorporated, Contract DAMD17-75-C-5040, U.S. Army Medical Research & Development Command, First Annual Report, Apr 1976.
48. Robinson, G. W. Rhodopsin cooperativity in visual response. *Vision Res* 16:35 (1975).
49. Connolly, J. A., Retinal photochemistry. In Research on the ocular effects of laser radiation. Technology Incorporated, Contract F41609-73-C-0017, USAF School of Aerospace Medicine, Twelfth Interim Technical Report, Mar 1976.
50. Nawrocki, A. D. and R. F. Lemberger. Unpublished results, 1975. (It should be noted that ray-tracing does not consider diffraction.)
51. Abrahamson, E. W. and J. R. Weisenfeld. The structure, spectra, and reactivity of visual pigments. In H. J. A. Dartnall (ed.). *Handbook of Sensory Physiology*, Vol. VII/T, Ch. 3 (and references cited therein). Berlin: Springer-Verlag, 1972.
52. Menger, E. L. (ed.). Special issue on The chemistry of vision. *Accts Chem Res* 8: Mar 1974.
53. Cone, R. A., and W. H. Cobbs, III. Rhodopsin cycle in the living eye of the rat. *Nature* 221:820 (1969).
54. Dowling, J. E. and R. L. Sidman. Inherited retinal dystrophy in the rat. *J Cell Biol* 14:73 (1962).
55. Fire, S. and W. P. Hanson. Optical second harmonic generation in biological systems. *Appl Opt* 10:2350 (1971).
56. Visilenko, L. S., V. P. Chabotaev and U. V. Troitskii. Visual observation of infrared laser emission. *Sov Phys JETP (English translation)* 21: 513 (1965).
57. Birks, J. B. *Photophysics of aromatic molecules*, pp. 62-83, London: Wiley-Interscience, 1970.
58. Connolly, J. S. Retinal photochemistry. In Research on the ocular effects of laser radiation. Technology Incorporated, Contract F41609-73-C-0017, USAF School of Aerospace Medicine, Draft Final Technical Report, Dec 1976.
59. Connolly, J. S., D. S. Gorman and G. R. Seely. Laser flash photolysis of chlorin and porphyrin systems. *Ann NY Acad Sci* 206:649 (1973).

BIBLIOGRAPHY

Arden, G. B., The excitation of photoreceptors. *Prog Biophys Mol Biol* 19(2): 373 (1969).

Bonting, S. J. The mechanism of the visual process. In D. R. Sanadi (ed.). *Current topics in bioenergetics*, 3:351 (1969).

Bridges, C. D. B. Biochemistry of vision. In C. N. Graymore (ed.). *Biochemistry of the eye*, ch. 9, London: Academic Press, 1970.

Cone, R. A. Early receptor potential: Photoreversible charge displacement of rhodopsin. *Science* 155:1128 (1967).

Dartnall, H. J. A., (ed.). *Handbook of sensory physiology*. Berlin: Springer-Verlag, 1972.

Vol. VII/1, Photochemistry of vision: See especially:

- Ch. 2, The chemistry of the visual pigments, R. A. Morton.
- Ch. 3, The structure spectra and reactivity of visual pigments, E. W. Abrahamson and J. R. Weisenfeld.
- Ch. 5, The behavior of visual pigments at low temperatures, T. Yoshizawa.
- Ch. 7, Physical changes induced by light in the rod outer segments of vertebrates, G. Falk and P. Fatt.
- Ch. 9, Visual pigments in man, W. A. H. Rushton.
- Ch. 10, The regeneration and renewal of visual pigment in vertebrates, Ch. Baumann.

Vol. VII/2, Physiology of photoreceptor organs: See especially:

- Ch. 5, The structure and reaction of visual pigments, A. Kropf.
- Ch. 16, Light and dark adaptation, P. Gouras.

Kuwabara, T. Surface structure of eye tissue. *Proc. of 3d Annual Scanning Electron Microscopy Symposium*, IITRI, Chicago, 1970.

Mainster, M. A. Retinol transport and regeneration of human cone photopigment. *Nature* 238:223 (1972).

Mainster, M. A., T. J. White and C. C. Stevens. Mathematical analysis of rhodopsin kinetics. *Vision Res* 11:435 (1971).

Moses, R. A. (ed.). *Adler's physiology of the eye*, 5th ed., Ch. 15, Photochemistry of vision. St. Louis: The C. V. Mosby Co., 1970.

Noell, W. K. Cellular physiology of the retina. *J Opt Soc Am* 53:36 (1963).

Rushton, W. A. H. Vision as a photic process, pp. 123-162. In A. C. Giese (ed.). *Photophysiology*, Vol. II. New York: Academic Press, 1964.

Wald, G. Molecular basis of visual excitation. *Science* 162:230 (1968).

Weale, R. A. Photochemistry and vision, pp. 1-45. In A. C. Giese (ed.). *Photophysiology*, Vol. IV. New York: Academic Press, 1968.

APPENDIX A DATA ANALYSIS

Statistical analyses of the data were performed using the method of probits¹. Preliminary probit calculations were carried out on a Wang 700B programmable calculator as described previously², and final analyses were conducted in the Biometrics Division, USAF School of Aerospace Medicine (SAM/BRD). The latter values are reported here.

For the 16 exposure sites in each eye, the powers (or energies) were equally spaced on a logarithmic scale from about half to twice the estimated threshold. The latter was obtained from prior experiments or, if necessary, from preliminary exposures, usually on one to four eyes. A log-normal distribution of dose was assumed because otherwise, on a linear scale the distribution curve of the experimental thresholds would be skewed; i.e., the probability is nil that an individual threshold will be zero, whereas there is a finite probability that a given threshold will be several times higher than the mean. Thus, by transforming the experimental laser powers (or energies) to a logarithmic scale, the probit analysis could be carried out assuming a Gaussian distribution function.

Because of general differences in pigmentation, age, and overall health of the subjects, we assume that the variability from eye to eye is greater than the variability among sites within a given macula. We further assume that the sensitivity levels (i.e., the threshold level for a burn) for all exposure sites in a given eye are randomly distributed across the macula, regardless of the specific location. Accordingly, a probit analysis was carried out for each eye, using a binary lesion/no-lesion determination for each of the 16 exposure sites. The result of each calculation is an ED50 which is defined as the laser power (or energy), incident on the cornea, that has a 50% probability of inducing macular damage at any site selected at random in the macula.

Each ED50 reported here is the geometric mean (i.e., arithmetic mean on a log scale) of the individual values for a given set of exposure parameters. The mean ED50, therefore, represents the 50% probability point for macular damage induced in any eye taken at random from the population. The upper and lower 95% confidence levels (UCL, LCL) are computed as standard 90% confidence limits on the mean (on a log scale) and then converted to dose units. Thus, UCL and LCL represent the 90% confidence interval for the ED50; i.e., the interval that should contain the true ED50 with 90% probability.

Preliminary probit analyses were carried out on all exposure sites, in all eyes exposed to a given set of conditions (pulsedwidth, pulse-repetition rate, pulse-train duration). Implicit in this combined-probit approach is the more restrictive assumption that the variability from eye to eye is no greater than the variability among sites within a given macula. There does not appear to be any *a priori* reason that this assumption should be valid. Nevertheless, we

1. Finney, D.J. Probit analysis, 2d ed. New York: Cambridge University Press, 1952.
2. Skeen, C.H., et al. Ocular effects of repetitive laser pulses. Technology Incorporated, Contract F41609-71-C-0018, USAF School of Aerospace Medicine, Final Report, June 1972.

found good agreement between the two sets of ED50's as well as their respective 90% Confidence Intervals, especially for large (≥ 10 eyes) sample populations.

The 90% Confidence Intervals reported here on experimentally determined ED50's are in general, within 5% of the respective ED50's. This narrow range of variation indicates only the precision of our data and not the accuracy. The reproducibility of retinal damage thresholds among different laboratories depends on factors such as equipment setup, system calibration, experimental procedures, animal care, and most importantly, the relative abilities of different observers to detect retinal lesions ophthalmoscopically. Thus, it is not unexpected that results of closely similar experiments, performed independently, have shown significant differences.

A more realistic estimate of the variability of retinal thresholds was obtained by fitting³ 15 experimental ED50's for a wavelength of 514.5 nm with a pulsewidth not less than 10 μ sec. The equation empirically fitted was:

$$\text{ED50(mW)} = 7.466t^{-.1502} + 1.030(10)^{-3} t^{-1}$$

where t is pulsewidth in seconds. The errors were assumed proportional, so that fitting was done taking logarithms of both sides of the equation as a first order approximation. The standard error thus obtained was 0.0945, which related approximately to an error rate of 24%. This estimate of standard error provides a more reasonable basis for computing confidence intervals than using the estimate of standard error from a single experimentally determined ED50. There is no adjustment for sample size when using this more realistic estimate of error.

This standard error is quite close to our estimated error of $\pm 20\%$ which is based on additivity of the possible sources of error in our measurements. It includes the biological variability from subject to subject, as expressed by the 90% Confidence Interval, which ranges from about $\pm 1\%$ to $\pm 7\%$. Taking the larger of these two as an upper limit, we add $\pm 10\%$ for calibration error and about $\pm 3\%$ for operational error. The calibration error contains the absolute error ($\pm 5\%$) of the energy measuring device (ballistic thermopile) and can also be considered an upper limit.

In summary, we believe the threshold values reported here to be accurate within a factor of about 25% and possibly within 20% of the stated value. As noted in the text, the agreement of our values with results reported by other investigators is, in general, quite satisfactory. A similar curve was obtained for neodymium based on seven experimental values. These two equations have been used to obtain predicted values at certain points where no experimental data exists. The tabled 90% Confidence Limits for these values are based on the estimates of the standard errors of predicted values from the fitted curves and are only approximate because of the nonlinearity of the equations.

3. McNee, R. C. Prediction of a single-pulse ED50. Unpublished report, USAF School of Aerospace Medicine (SAM/BRD), Jun 1977.